AFIT/GEE/ENP/94S-02

EXPERIMENT USING INFRARED SPECTROSCOPY TO STUDY THE EFFECT OF SOIL CHARACTERISTICS UPON THE RATE OF TRICHLOROETHYLENE DESORPTION

THESIS

Benjamin T. Kindt, Captain, USAF

AFIT/GEE/ENP/94S-02

AFIT/GEE/ENP/94S-02

EXPERIMENT USING INFRARED SPECTROSCOPY TO STUDY THE EFFECT OF SOIL CHARACTERISTICS UPON THE RATE OF TRICHLOROETHYLENE DESORPTION

THESIS

Presented to the Faculty of the School of Engineering

of the Air Force Institute of Technology

Air University

In Partial Fulfillment of the

Requirements for the Degree of

Master of Science in Engineering and Environmental Management

Benjamin T. Kindt, B.S., M.B.A.

Captain, USAF

September 1994

Disclaimer Statement

The views expressed in this thesis are those of the author and do not reflect the official policy or position of the Department of Defense or the United States Government.

Acknowledgments

I wish to thank my advisor, Major Glenn Perram, for his guidance, patience, and leadership. I also give thanks to my colleagues Captain Peter La Puma and Lieutenant Abdellatif Tares for their assistance and teamwork throughout the completion of this research. Above all, I wish to thank my wife, Margaret, for her constant love and support without which this document would not have been possible.

Table of Contents

List of Figures

List of Figures

List of Tables

Abstract

This research investigated the influence of soil characteristics on the desorption of trichloroethylene (TCE). TCE is one of the most common contaminants at Superfund sites. Unfortunately, extraction of TCE from contaminated soils has been hindered by its slow and poorly understood desorption from soil particles.

The rate and progress of desorption of TCE from seven types of soil with varying particle diameters and elemental compositions was measured using optical absorption techniques. Fitting the data to the Langmuir Isotherm functional form predicted in the literature yielded parameters for the desorption rate and total amount of desorption from each soil type. These parameters were compared to the characteristics of the soil samples to determine if any correlation existed.

Soil characteristics appeared to have a significant influence on the desorption of TCE. Both the rate of desorption and the total amount of desorption showed a strong negative correlation with the particle diameter of the soils. Additionally, the elemental composition of the soil appeared to have a significant effect on the desorption phenomena.

I. Introduction

Although considerable research has been conducted regarding volatile organic contaminant (VOC) behavior within groundwater, relatively little work has been done to increase understanding of the slow VOC desorption mechanism within the vadose zone. The overall desorption phenomena is poorly understood, in part, due to the many factors that appear to influence desorption rates. The physical characteristics of the contaminated soil, the soil temperature, and the length of contamination all appear to play a significant role in defining the r·e at which desorption will occur (Smith, 1990: 682).

In order to increase the understanding of the desorption phenomena in vadose zone contaminated soils, this thesis evaluated the influence of soil characteristics upon the desorption rate of trichloroethylene (TCE) using optical techniques. Observations were made of the desorption phenomena from seven types of well characterized soil contaminated for a specific amount of time and held at a constant temperature.

There were three primary objectives of this thesis. The first objective was to determine if soil characteristics had any influence on the rate and/or progress of desorption of TCE, and if so, to provide insight into what the nature of these influences might be. The second objective of the thesis was to determine whether currently held theories regarding the microscopic mechanism of contaminant desorption agreed with actual observations made in the laboratory under controlled conditions. Finally, the third objective was to evaluate the utility of using optical techniques to study microscopic chemical processes in the environment.

To accomplish these objectives, the thesis was performed in three

distinct phases. The first phase involved the measurement of the infrared absorption spectrum of gas phase trichloroethylene (TCE) at high resolution (0.02 cm^{-1}) to enable the design of an optical measurement apparatus. The second phase involved the determination of the absorption cross-sectional area of a vapor phase TCE molecule. Knowledge of this property was necessary to enable calculation of the concentration of TCE in a sample placed within the optical measurement apparatus. Finally, the third phase involved the use of the optical measurement apparatus to measure the rate and progress of TCE desorption from seven types of soil.

The results of this thesis may be important to several groups of professionals. By further applying the results of this thesis, engineers and scientists may gain a better understanding of the behavior of TCE in the environment. Analysis of the effects of soil characteristics upon TCE desorption may allow the construction of more accurate models to predict the rate and progress of contaminant transport. This knowledge may aid engineers in the development of more effective remediation techniques to deal with the problem of TCE slow desorption within the vadose zone. Additionally, increased understanding of desorption may allow project managers to make more realistic estimates of the time and cost involved at TCE contaminated sites using current remedial technologies. Finally, this thesis may provide researchers additional insight into the utility of using optical measurement techniques for future environmental research applications.

II. Background

2.1 General Background.

TCE has become the primary VOC in the soil and groundwater of the United States (Lewis, 1991: 2). Widely used as an industrial and domestic solvent for decades, TCE has contaminated over 35% of the nation's Superfund sites (Siegrist, 1992: 3-4). Within the Air Force, TCE has been used extensively for cleaning metal and electronic parts and degreasing aircraft components. Additionally, at Air Force installations worldwide, where TCE has been used throughout maintenance and industrial operations for decades, TCE has been commonly found contaminating the soil and groundwater (Siegrist, 1992: 3). Consequently, the Air Force has invested hundreds of millions of dollars annually as part of its Installation Restoration Program (IRP) in an effort to remediate TCE contamination at these sites.

The TCE contamination in the soil and groundwater at these sites has been a major health concern. Until the mid-1970's, TCE was generally considered harmless to humans and was even used as a medical anesthetic and food additive (Lewis, 1992: 3352). In 1976, a study identified TCE as a suspected human carcinogen which prompted the EPA to list TCE on its hazardous substances list (Lewis, 1992: 3353). Further study by the EPA resulted in "discarded" TCE being listed as a toxic waste in the Federal hazardous waste disposal regulations (40 CFR 261.33). As part of its effort to ensure the protection of the nation's drinking water supply from carcinogenic agents, the EPA established a safe drinking water maximum contaminant level (MCL) of 5 parts per billion (ppb) for TCE (Bourg, 1992: 365).

Exposure to TCE also poses non-cancer related hazards. For example, toxicity testing has shown TCE to have adverse health effects

when introduced to subjects through oral, respiratory, and dermal exposure routes. High concentrations of TCE may also cause skin and eye irritation, hepatitis, or depression of the central nervous system (Lewis, 1992: 3353).

The physical properties of TCE have been well characterized (Lewis, 1992: 3352-3353). Specific properties of TCE are listed in Table 1. The density of TCE is greater that that of water at 20 °C, indicating that TCE will tend to sink to the bottom of a water/TCE mixture. Additionally, TCE has a relatively low molecular weight and high vapor pressure, indicating that the chemical is highly volatile.

TABLE 1

PHYSICAL PROPERTIES OF TCE

Property	Value	Units
Physical State (@ 15°C and 1 atm)	Liquid	
Chemical Formula	$ClHC=CCL_2$	
Molecular Weight	131.39	amu
Density (@ 20°C)	1.46	g/cm^3
Liquid Surface Tension (@ 20°C)	0.0293	N/m
Vapor Specific Gravity	4.5	g/cm^3
Vapor Pressure (@ 20 °C)	58.0	torr
Latent Heat of Vaporization	$2.4x10^5$	J/kg
Viscosity	0.57	cP
Solubility (@ 20C)	0.7	g/liter
Henry's Constant	0.232	unitless
Partition Coefficient	0.199	ml/g
EPA Maximum Contaminant Level (MCL)	0.005	mg/liter
Temperature Characteristics		
Auto-Ignition Temperature	788.0	°F
Flash Point	89.6	°C
Boiling Point	86.7	°C
Melting Point	-70.0	°C
Freezing Point	-86.8	°C

(Lewis, 1992: 3352-3353).

2.2 The Behavior of TCE in the Environment.

When a dense (higher specific gravity than water), non-aqueous phase (relatively insoluble in water) liquid (DNAPL) such as TCE is released to the environment, it tends to migrate rapidly through soils, leaving behind droplets of contaminant in the voids between the soil particles (Bourg, 1992: 365). These droplets may become liquid, vapor, or may sorb into the solid soil particles themselves. The nature of the partitioning of the contaminant among these three general states is complex and dependent on many factors such as environmental conditions (temperature, hydrodynamics, surface features, humidity), VOC properties (solubility, vapor pressure, Henry's constant, boiling point), soil properties (organic carbon content, particle size, bulk density, percent moisture), and microbiological factors (Lewis, 1991: 3-7). The equilibrium partitioning in the soil matrix among the gas, liquid, and sorbed phases may be described by the following relationship (Siegrist, 1992: 3):

$$C_\tau = a\, C_v\, \rho_b + \theta\, C_L / \rho_b + C_s \qquad (1)$$

where:

C_τ = the total VOC concentration per mass of dry soil ($\mu g/g$).

C_v = the vapor phase volumetric VOC concentration ($\mu g/cm^3$).

C_L = the liquid phase volumetric VOC concentration ($\mu g/cm^3$).

C_s = the sorbed phase concentration per mass of dry soil ($\mu g/g$).

ρ_b = the soil density (g/cm^3).

θ = the soil water content (cm^3/cm^3).

a = the soil air content (cm^3/cm^3).

The contaminant concentration in the sorbed phase may be related to the liquid phase concentration using the Freundlich Isotherm:

$$C_S = K C_L^{1/n} \quad (2)$$

where:

K = the sorbed/liquid partition coefficient.

n = an empirical constant.

The value of the sorbed/liquid partition coefficient is linearly dependent on the water solubility of the VOC and the organic content of the contaminated soil (Siegrist, 1992: 3). When the exponent term 1/n is approximately equal to one, it implies that the amount of contaminant sorbed into the soil is linearly related to the concentration of liquid contaminant surrounding the soil (Rogers, 1980: 458).

In the unsaturated soils of the vadose zone, the liquid and vapor phase concentrations may be related using Henry's Law:

$$C_V = K_H C_L \quad (3)$$

where:

K_H = Henry's constant for the contaminant.

Another relationship may be used to relate the sorbed phase concentration to that in the gas phase. This relationship is called the Langmuir Isotherm and is as follows (Laidler, 1965: 264-274):

$$\beta = K_L C_V / (1 + K_L C_V) \quad (4)$$

where:

β = the fraction of a the surface area of the soil that is covered by the VOC contaminant. β is dependent on the geometry of the soil particle.

K_L = the ratio of contaminant adsorption and desorption rate coefficient.

Under equilibrium conditions, the vast majority of the TCE in the vadose zone will reside in the solid phase (Siegrist, 1992: 5-7). Even after remediation of vapor and liquid phase contaminants in the vadose zone using a vapor extraction system, the remaining solid-phase contaminants may represent up to 90% of the total contaminant volume (Travis, 1992: 1887). It is clear that on a volumetric basis, almost all of the TCE in the vadose zone becomes firmly trapped within the soil particles and is only released through desorption over a long period of time (Barcelona, 1993: 5).

Additional insight into the desorption mechanism may be gained by looking at a kinetic model of the Langmuir Isotherm. If desorption of TCE from soil is represented by the following equation:

$$\text{Sorbed TCE} \xrightarrow{K_d} \text{TCE} + \text{vacant site on soil} \qquad (5)$$

where:

K_d = the rate coefficient for desorption.

It is important to note that in the above model the effects of reabsorption of TCE by the soil sorption sites is assumed to be negligible. This appears to be a reasonable assumption in conditions where all liquid or vapor phase TCE external to the soil particles has

already been extracted from the soil matrix and only the sorbed phase remains. The desorption/absorption process will proceed solely in the desorption direction until an equilibrium condition is reached, with very little reabsorption occurring.

Analyzing the above model, it can be said that the concentration of TCE in the vapor phase (having been desorbed from the soil) as a function of time then is as follows:

$$\frac{d\,[TCE]}{dt} = K_d\,\theta \tag{6}$$

where:

K_d = the rate coefficient for desorption $\left(\frac{\text{molecules}}{\text{cm}^3\ \text{sec}}\right)$.

$$\theta = \frac{\#\ \text{of sorbtion sites occupied by TCE molecules}}{\text{total}\ \#\ \text{of sorbtion sites}}.$$

Also, change in the amount of occupied sorption sites in the soil over time may be represented by:

$$\frac{d\theta}{dt} = -\frac{K_d}{\mu}\,\theta \tag{7}$$

where:

μ = the concentration of TCE initially in soil $\left(\frac{\text{molecules}}{\text{cm}^3}\right)$.

Thus, the change in the number of gas phase TCE molecules is inversely proportional to the change in the number of occupied sorption sites in

the soil. Integrating the above equation results in:

$$\theta(t) = \theta_0 e^{-\frac{K_d}{\mu} t} \quad (8)$$

where:

θ_0 = $\frac{\text{\# of sorbtion sites occupied by TCE molecules}}{\text{total \# of sorbtion sites}}$ at time t = 0.

If the assumption is made that initially the soil is completely saturated with the contaminant, and all available sorption sites are initially occupied, θ_o is assumed to be 1. Applying this assumption and substituting Equation 8 into Equation 6 leads to:

$$\frac{d[TCE]}{dt} = K_d e^{-\frac{K_d}{\mu} t} \quad (9)$$

Integrating this expression with respect to time yields:

$$TCE(t) = \mu (1 - e^{-\frac{K_d}{\mu} t}) \quad (10)$$

The desorption of TCE from soil is expected to behave according to Equation 10. Thus, the desorption rate is expected to be initially high, but gradually level off to zero as the total desorption time increases. Examination of Equation 10 indicates that the rate and progress of TCE desorption from soil will be dependent upon two parameters: μ and K_d. The value of μ will determine the amount of TCE

that will ultimately be desorbed from the soil after an infinite amount of time has passed. The value of K_d will determine the rate at which the desorption will occur and how quickly the asymptotic limit of desorption, μ, will be approached.

A number of environmental factors appear to influence VOC sorption. First, the amount of water present in the vadose zone soil matrix plays a significant role in the VOC sorption mechanism. In dry soils, large amounts of TCE appear to be readily adsorbed by soil particles. In soils with moderate humidity (one to five monolayers of water molecules on the soil particles), water appears to sorb into the soil particles, restricting adsorption of TCE (Chiou, 1990: 149-152). In soils heavily saturated with water (over five monolayers of water molecules), some TCE will be dissolved into the water and be sorbed as an aqueous phase solution (Ong, 1991: 182-184).

Second, there is conflicting research as to the effect of soil pH upon the desorption of VOCs. One study measuring the desorption rate from soil contaminated with TCE for 18 years concluded that pH had a negligible effect on the desorption rate. The study concluded that this result was expected since TCE is a non-polar hydrocarbon and thus should not be affected by changes in pH (Pavlostathis, 1991: 274). Another study evaluating the effects on the sorption of TCE into montmorillite clay over a 36-hour period found a strong correlation. The results of this study indicated that sorption was maximized at a pH of 4 with sorption dropping off sharply at pHs above and below 4 (Estes, 1988: 377-380). Although the differences between the two studies remains unexplained, it is important to note that the soil in the second experiment was contaminated for only 4 days while the soil in the first experiment had been contaminated for 18 years. The length of contamination may have had an affect on the nature of the TCE

entrainment within the soil particles.

Third, the surface area of a sample's soil particles appears to effect the VOC sorption mechanism. The smaller a particle is in volume, the greater amount of surface area a given mass of these particles will have. The greater the amount of surface area, the greater the amount of surface/TCE interactions will occur. Hence, sorption will tend to be more pronounced in soils with a small particle size. The effect appears to be especially significant in dry soils where water molecules are not competing for the available soil pore spaces (Ong, 1991: 183).

Fourth, although a detailed study has not been identified addressing the effects of temperature upon the desorption of TCE, there is evidence that a significant relationship may exist (Chiou, 1990: 142). The desorption of polycyclic aromatic hydrocarbons (PAHs) from loamy sand has been shown to be much faster when the sample temperature is increased (Maliszewska, 1992: 15-16). Another study regarding the desorption of the pesticide parathion from water saturated soil indicated that temperature changes will affect the nature of the water/contaminant competition for available pore spaces depending on the heat of absorption of the contaminant (Chiou, 1990: 142).

Fifth, the length of time the vadose zone has been contaminated appears to play a significant role in defining how the desorption process will proceed (Pavlostathis, 1991: 274). Research has shown that the longer a contaminant remains in contact with the soil, the greater the volume of the contaminant will become entrained in the solid phase (Smith, 1990: 382). Additionally, the longer a soil sample has been exposed to TCE, the slower the rate of desorption will be (Pavlostathis, 1992: 536). This same research indicated that the type of soil that has been contaminated appears to have no significant effect on the rate of the sorption phenomena (Pavlostathis, 1992: 535).

2.3 Current Solutions to TCE Contamination.

Releases of liquid TCE to the environment typically result in contamination of the unsaturated (from the soil surface to the top of the water table) and the saturated (below the top of the water table) zones (Bourg, 1992: 365). Saturated zone contamination is usually treated as posing the most immediate threat to human health (Masters, 1991: 160-164). This policy is due to the fact that groundwater remains an important source of drinking water for many parts of the country; thus a contaminated aquifer could cause rapid, widespread human exposure. Additionally, contaminated groundwater flowing through the saturated zone can serve as a relatively rapid transport mechanism to spread the area of contamination, creating a more difficult and expensive cleanup problem (Bourg, 1992: 365).

Due to the immediate dangers posed by saturated zone contamination, the majority of remediation efforts have focused on this area (Bourg, 1992: 365). Efforts to cleanup groundwater have typically consisted of pumping the contaminated groundwater to the surface through installed extraction wells, treating the water on the surface, and returning the remediated water to the saturated zone via installed injection wells (Goltz, 1991: 547). Although many of these pump-and-treat systems have shown high initial contaminant extraction rates, the efficiency of the systems typically decreases to some limiting asymptotic value (Goltz, 1991: 547). Initially, a large amount of the contaminant is extracted by the system in a short period of time. However, as treatment continues, the efficiency of the system decreases and contaminants are extracted at a decreasing rate. The reduced pumping efficiency phenomena tends to extend the amount of time required to pump and treat the required contaminant volume from the groundwater,

increasing the cleanup cost and time (Reeder, 1993: 2).

Within the vadose zone, VOCs partition themselves among five different phases (Travis, 1992: 1886). First, the contaminants may exist as a free-liquid phase suspended among the soil particles. Second, the contaminant may exist as a vapor occupying void spaces between the soil particles. Third, if there is water present in the soil matrix, the contaminant may dissolve into the water and form an aqueous phase among the soil particles. Fourth, the contaminant be absorbed onto the surface of soil particles. Finally, fifth, the contaminant may be absorbed deeply into the soil particles and trapped in the interior particle pore spaces. The fourth and fifth phases are sometimes collectively referred to as the solid or sorbed phase. Recent research indicates that over time, more than 50% of the VOC contaminants in the unsaturated zone may partition to the deep interior of the soil particles (Siegrist, 1992: 3).

The limitations of pump-and-treat technology are believed to be caused by contaminants continuously and slowly desorbing from the interior of soil particles in the vadose zone and flowing downward to the saturated zone (Tognotti, 1991: 104). The gradual desorption and flow of contaminants from the vadose zone may continue for years or even decades (Pignatello, 1990: 1108). The continued recontamination of the aquifer caused by slow desorption frustrates and may even reverse groundwater remediation efforts (Reeder, 1993: 2). On sites previously treated and achieving the regulatory standards for cleanup, the slow sorption phenomena may over time cause TCE concentration levels in the groundwater to rise back above regulatory limits, requiring a reopening of the site.

Efforts to remediate the vadose zone directly and thus halt the slow sorption phenomena have typically applied either vapor extraction

or biological treatment techniques (Pavostathis, 1991: 274), (Travis, 1992: 1886). These systems seek to remove contamination from all five phases of VOC within the vadose zone soil matrix and thereby prevent future recontamination of the aquifer below. Vapor extraction involves forcing large volumes of surface air through the contaminated soil in an effort to volatilize the trapped contaminant. The volatilized contaminant is then collected and treated at the surface (Travis, 1992: 1886). Biological treatment involves application of nutrients and oxygen to the vadose zone to stimulate and accelerate the biological mineralization of the contaminants. Through this process the contaminants are broken down by microbial activity into harmless carbon dioxide and oxygen molecules (Pavlostathis, 1991: 274). Although both technologies have proven highly effective in treating vapor, aqueous, and liquid phase contaminants in the vadose zone, neither technique has proven successful at treating either the surface sorbed or the deeply sorbed phase contaminants (Pignatello, 1990: 1107-1108).

2.4 Contamination Measurement Issues.

Compounding the problem of successfully treating sorbed phase contaminants in the vadose zone is limited effectiveness offered by current measurement techniques. The analytical procedure approved by the EPA for measuring VOCs in soil samples from the vadose zone is the "purge and trap" method (Sawhney, 1988: 150). Unfortunately, studies have shown that this method is unable to detect sorbed phase contaminants and therefore frequently identifies less than 50% of the contamination present in soil samples (Travis, 1992: 1887). During vapor extraction and biological treatment operations, the purge and trap method is frequently used to measure the success of the remedial action. However, using this analytical procedure, over 50% of the contamination

at the site may remain undetected and untreated when the project is classified as successful (Siegrist, 1992: 11). The remaining sorbed contamination may later desorb into the saturated zone creating a hazard to human health and the environment.

One potential alternative measurement method for vadose zone sorbed contamination is the use of infrared spectroscopic optical techniques (Reeder, 1993: 84). TCE absorbs light at particular, well-defined wavelengths. By choosing a wavelength at which TCE strongly absorbs light and by emitting light from an infrared source of known intensity across a contaminated sample, one may measure the amount of light at that wavelength absorbed by the sample. Using this optical measurement technique, one may readily calculate the amount of TCE present in the sample.

2.5 Optical Measurement of TCE Desorption.

All molecules emit and absorb electromagnetic energy. Depending on its structure and composition, a particular molecule may absorb and emit electromagnetic energy waves more efficiently at some wavelengths than at others. The various numbers and types of bonds a molecule has defines the directions and frequencies in which it may rotate or vibrate. If a molecule rotates or vibrates at a particular frequency, then it will tend to absorb energy at that frequency. For example, TCE is very strongly absorptive of energy from light at a wavelength of 3080 cm^{-1} (Sadtler, 1977: 1307), but absorbs almost no energy from light near 3000 cm^{-1}. The unique structure of the TCE molecule defines the manner in which it rotates and vibrates making it receptive to energy at 3080 cm^{-1} but not receptive to light at other nearby wavelengths.

Additional insight into the interaction between electromagnetic energy and TCE may be gained by examining the case of an enclosed sample

of TCE vapor through which a beam of light is shown. A drawing of this model is presented in Figure 1. Among the photons of the light beam traveling through the contaminated sample, there will be a portion possessing a frequency that TCE absorbs. For a particular number of TCE molecules within the sample and a particular number of photons traveling though the sample at the proper frequency, there will be a probability that a molecule/photon "impact" will occur and that the molecule will absorb the energy of the photon.

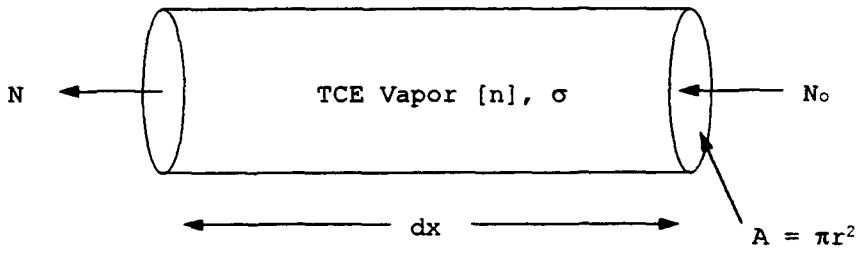

Figure 1. TCE Optical Absorbtion Model

Each TCE molecule has an effective cross-sectional area, σ. This property represents the area of an individual TCE molecule at a right angle to the direction of photon flow (i.e. the path of the light beam). Hence, the probability of a TCE/photon interaction is proportional to σ. Using this relationship:

N = the number of photons not absorbed and leaving the sample.

dN = the number of photons absorbed by TCE in the sample.

dx = the length of the contaminated sample through which the photons will travel, cm.

A = the cross-sectional area of the sample (πr^2), cm^2.

σ = the cross-section of TCE for optical absorption (cm^2/molecule).

n = the number of TCE molecules within the sample per unit volume (molecule/cm^3), each having cross-sectional area, σ.

The ratio of the number of absorbed photons to the number of photons not absorbed (passing through the sample, unaffected by the TCE), (dN/N), is equal to the ratio of the total sample TCE cross-sectional area, ($n\sigma$ Adx), to the sample cross-sectional area (Serway, 1983: 1068). The relationship may be presented as follows:

$$-\frac{dN}{N} = \frac{n\ A\ \sigma\ dx}{A} \tag{11}$$

or

$$-\frac{dN}{N} = n\ \sigma\ dx \tag{12}$$

The negative sign associated with the dN/N term indicates that the quantity of photons in the light beam is reduced as photons are absorbed by TCE molecules. Integrating the above expression over the length of the sample (where $N = N_0$ at $x = 0$) we get:

$$\int_{N_o}^{N} \frac{dN}{N} = -\ n\ \sigma \int_{0}^{x} dx \tag{13}$$

Integrating this expression leads to:

$$\ln\left(\frac{N}{N_o}\right) = - n \sigma x \tag{14}$$

or

$$N = N_o e^{(-\sigma n x)} \tag{15}$$

Analyzing this expression, we see that the number of photons that are absorbed increases exponentially with the length of the path they must travel through a TCE contaminated sample (Serway, 1983: 1068). Also, increasing the concentration of TCE within the sample results in a proportional exponential decrease in the number of photons able to pass throughout the sample unabsorbed.

If the path length of the sample is held constant, the only remaining variable in Equation 15 is the number of TCE molecules, n. Using the above sample (maintaining a constant path length) containing an unknown concentration of TCE and measuring both the incident and transmitted light intensities (typically measured in units of mvolts using optical detectors), enables the use Beer's Law to calculate the concentration of TCE within the cell. The Beer's Law equation is as follows:

$$I_t = I_o e^{-\sigma l N} \tag{16}$$

where:

I_t = the transmitted intensity (mvolts).

I_o = the incident intensity (mvolts).

l = the optical path length (cm).

N = the concentration of TCE in the sample (molecule/cm^3).

Thus, according to Beer's Law, infrared radiation of a known intensity transmitted through a TCE contaminated sample of a known length will decay exponentially (Serway, 1983: 1068). Solving for the TCE concentration, N:

$$N = -\frac{1}{\sigma l} \ln\left[\frac{I_t}{I_o}\right] \tag{17}$$

Therefore, in a sample with fixed length, using TCE with a well-characterized cross-section, one may determine the concentration of TCE molecules by measuring the decay in intensity of a light beam transmitted through the sample.

III. The Experiment

3.1 Introduction.

To accomplish the three objectives of the thesis, the experiment was performed in three distinct phases. The first phase involved evaluation of the light absorption properties of TCE using an infrared spectroscopic interferometer. Using this information, an optical bandpass filter was designed to screen out all light except within a frequency range where TCE strongly absorbed electromagnetic energy. This filter was subsequently included as a primary component of the apparatus used in Phases Two and Three. Phase Two involved constructing the experimental apparatus to be used in Phases Two and Three and using the apparatus to determine the optical absorption cross-section of a vapor-phase TCE molecule. Finally, Phase Three involved the use of the apparatus and the data from Phase Two to measure, over time, the TCE desorption phenomena from seven well-characterized soils. Using this data, attempts where made to fit the data to a functional form predicted in the literature for contaminant desorption from soil (the Langmuir Isotherm) and to determine if the fitted parameters of the function correlated with soil characteristics.

3.2 Phase One: Evaluation and Analysis of the TCE Absorption Spectrum.

3.2.1 Purpose. The purpose of Phase One was to select a narrow frequency range within which TCE molecules (and not potentially interfering water molecules and atmosphere) strongly absorbed electromagnetic energy. The selection of this range enabled the subsequent design of an optical filter that only allowed light within

the selected frequency range to pass. This filter was subsequently included in the measurement apparatus used to accomplish Phases Two and Three of the experiment.

Phases Two and Three both involved measurement of the change in intensity experienced by a beam of light passing through a sample of TCE. As discussed in Chapter 2, molecules (TCE, water, etc.) absorb energy from light at certain discrete frequencies depending on their particular molecular structure. Since this thesis studied the behavior of TCE, only changes in light intensity caused by TCE energy absorption were desired to be measured. Therefore, it was necessary to isolate a narrow frequency range within which TCE was strongly absorptive and water and atmosphere were not absorptive (in order to screen out interference from absorption by non-TCE molecules within the sample). Measuring intensity only within this isolated frequency range allowed identification of the amount of energy absorption by TCE while screening out other changes to the beam intensity caused by other molecules. The filter designed from the data gathered in Phase One enabled this isolation to occur.

3.2.2 Equipment. The primary piece of equipment used to accomplish Phase One was the Bomem DA-8 Fourier Transform Spectrometer. Samples were placed in a glass cylinder, 2 inches in diameter, with calcium fluoride windows fastened to each end. The sample container was evacuated (to $< 10^{-4}$ torr) to eliminate atmospheric interference and then filled with the sample to be evaluated. A functional diagram of the Bomem DA-8 is shown in Figure 2.

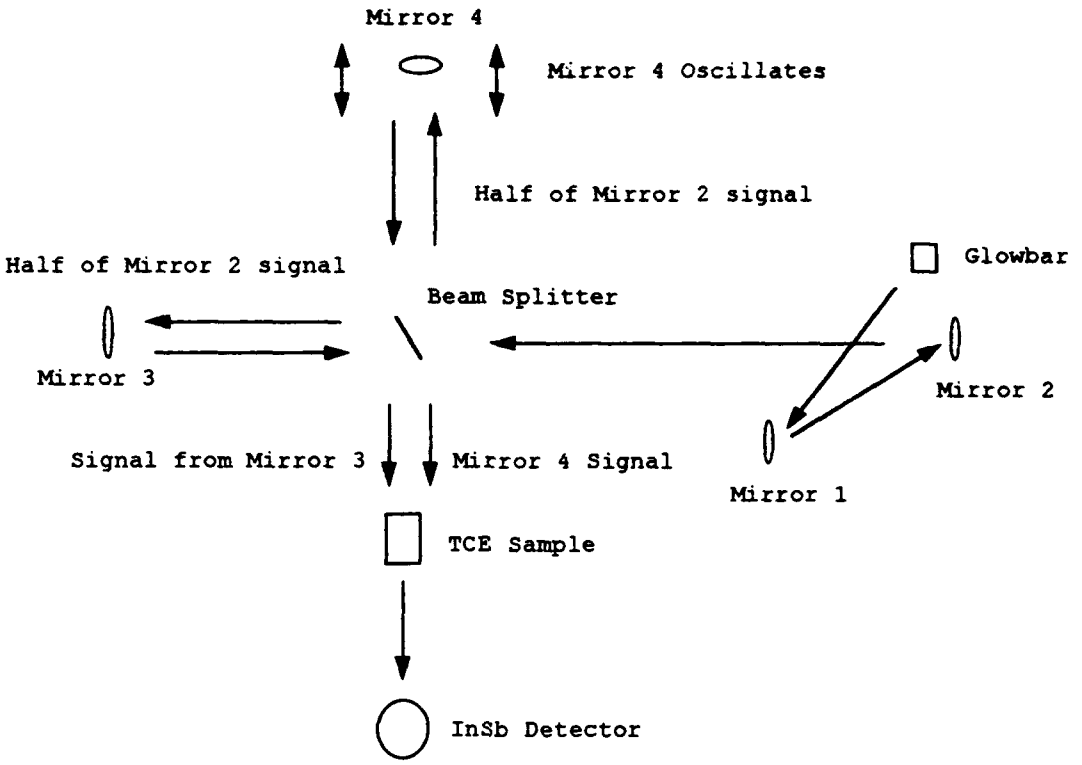

Figure 2. Functional Diagram of Bomem DA-8

3.2.3 Procedure. First, a low resolution interferogram of TCE vapor was generated using the Bomem DA-8. Additionally, a scan of the empty cell was performed and analyzed in the same manner to subtract any signal losses caused by the apparatus or calcium fluoride windows. Next, a Fourier transform of the TCE interferogram was calculated and analyzed to determine a frequency range where TCE strongly absorbed electromagnetic energy. Using this information, a high resolution (0.02 cm-1) scan was then performed on the TCE vapor in the strongly absorptive region. This scan was then compared to water vapor and atmosphere absorption characteristics reported in the literature

(Sadtler, 1977: 45054). This comparison was used to determine if water and/or atmospheric gases also were absorptive within the selected frequency range. If water or atmospheric gases absorbed energy within the same range, other frequency ranges where TCE strongly absorbed were evaluated until a range was identified within which TCE strongly absorbed and water and atmosphere did not absorb.

Upon identification of a frequency range where only TCE strongly absorbed, a band pass filter was designed and specified to closely match the same range. However, due to cost considerations the actual design of the filter actually exceeded the selected TCE absorption range, allowing surrounding frequencies, where neither TCE nor water or atmosphere absorbed, to pass. The correction required to account for this excess frequency transmission is discussed in the next chapter.

3.3 Phase Two: Determination of the Optical Cross-Section of TCE.

3.3.1 Purpose. The purpose of Phase Two was to determine the optical absorption cross-section of vapor-phase TCE molecules to enable application of Beer's Law (Equation 16) to calculate the concentration of TCE a sample cell (as described in Chapter 2).

3.3.2 Equipment. A schematic diagram of the experimental apparatus used in Phase Two is shown in Figure 3.

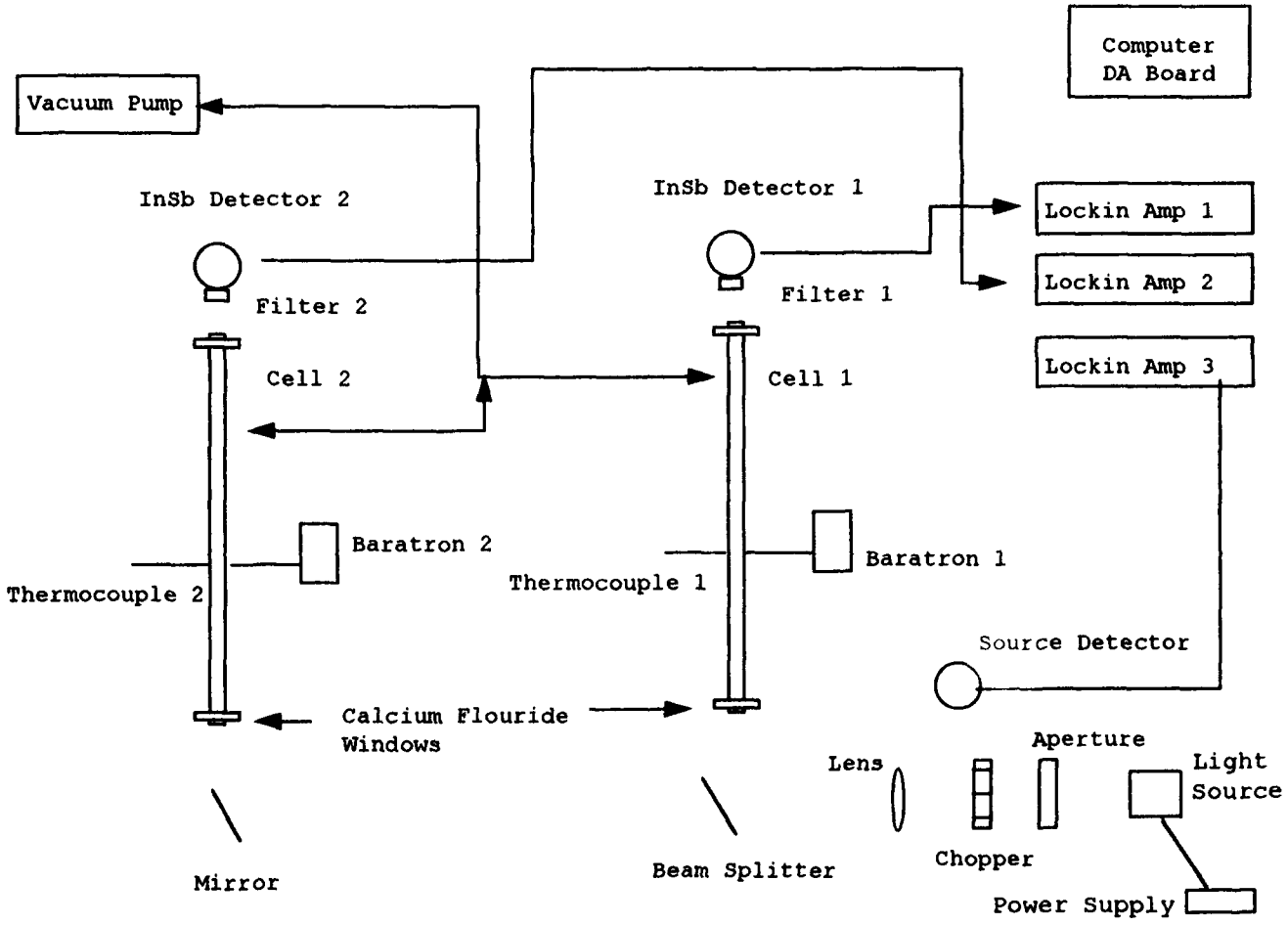

Figure 3. Schematic Diagram of Experiment Apparatus

The apparatus included the following components:

Light Source and Power Supply: The light source was a quartz-halogen glowbar lamp placed in a flat black, cylindrical mounting. The light source was oriented such that the signal was directed towards the adjacent aperture. Power was provided to the light source from a 12 volt, 60 hertz power supply.

Aperture: A flat black adjustable aperture was placed adjacent to the light source to narrow the beam transmitted to the adjacent optical chopper.

Optical Chopper: An optical chopper with an associated electrical motor and controller was placed after the aperture to impart a specific frequency to the light transmitted to the sample cells. The controller was a Model SR-540 Chopper Controller Device manufactured by Stanford Research Systems (SRS). Throughout the experiment, the chopper was set to rotate at a frequency of 24 hertz. This frequency value was output to the SR-510 Lock-In Amplifiers (discussed below). By giving the light beam a specific frequency and providing that frequency to the Lock-In Amplifiers, the amplifiers were able to eliminate stray light signals from other sources in the laboratory that might have interfered with the experiment.

Lens: A lens was positioned after the optical chopper to further narrow and focus the light beam. This allowed the beam to be focused enough to pass through the 1/2 inch diameter sample cells (discussed below) and to be focused upon the infrared detectors (also discussed below) at the end of the optical path.

Source Detector: A Hamamatsu room temperature, silicon photodiode detector was placed adjacent to the lens, facing the light source. The function of the source detector was to measure variations in the light beam's intensity over time, independent of the beam's interaction with the sample cells. Such variations could have been caused by properties of the light source itself, electrical power cycling, or disturbances in the laboratory. The voltage response from the source detector was output to lockin-amplifier three. Upon completion of Phase 2 and Phase 3 runs, the source detector's output was evaluated to determine if a variation of source intensity did occur. If such a variation occurred, the signal output from the indium antimonide detectors was corrected accordingly.

Beam Splitter: Since the light source is oriented perpendicular to the detectors (as shown in Figure 3), a beam splitter was required to reflect 50% of the light signal to the first sample cell and allow the remaining 50% to travel to the adjacent mirror to be reflected through the second sample cell.

Calcium Fluoride Windows: Transparent windows made of calcium fluoride were fastened to both ends of the sample cells using a two-part, low vapor pressure resin. Calcium fluoride was selected as the window material because of its favorable transparency to the infrared energy that was transmitted through the cell.

Sample Cells: Each sample cell was a T-shaped, one half inch diameter, hollow glass tube open on each of its three ends. Each of the ends was fitted with a one half inch Cajon Tube Fitting designed for sealing

glass tubing under vacuum. The fittings were manufactured of Type 316 stainless steel. The fittings were placed on the outside of the glass tubing and when tightened, fastened a teflon o-ring securely against the glass. The two open ends on the long portion of the sample cells were both connected by fittings to one inch long, one half inch diameter, straight glass tubes with a calcium fluoride window fastened to their ends. Thus, both ends of the long, straight portion of the sample cells were effectively sealed with calcium fluoride windows. The short portion of each sample cell was sealed with a fitting leading to the vacuum pump. The thermocouple was inserted through this fitting to enable temperature measurement.

Baratron Pressure Transducers: A Baratron pressure transducer was attached to each sample cell to monitor the internal pressure in each cell. The pressure transducer on cell one was a Type 122A, and the pressure transducer on cell two was a Type 221A. Both units were adjusted to measure pressure in units of torr within a range of 0 to 100 torr. Each unit provided a voltage signal proportional to its pressure measurement to the data acquisition board placed in the computer (discussed below).

Vacuum Pump: A 3/4 horsepower vacuum pump was connected to the apparatus to enable evacuation of the sample cells. The apparatus was designed such that each cell could be evacuated independently or simultaneously.

Thermocouples: A gas phase thermocouple was connected to each sample cell to enable temperature measurement internal to the cells. The thermocouples output a voltage proportional to the temperatures within

each cell which was then transmitted to the data acquisition board.

Optical Bandpass Filters: The optical bandpass filters designed at the end of Phase One were fastened to the front of the indium antimonide detectors. The purpose of the filters was to ensure that only the frequency range identified in Phase One would be transmitted to the detectors. Therefore, when measuring changes in the intensity readings measured by the detectors, only changes in intensity within the desired frequency range would be reported. The design and specifications of the filters will be discussed in the Phase One section of Chapter 4.

Indium Antimonide (InSb) Detectors: The two InSb detectors were used to measure the intensity of the signal transmitted after passing through the optical path, the sample cells, and the band pass filters. Each detector generated a voltage output proportional to the intensity of photons incident upon its detection surface. Both detectors were EE&G Judson model J10D-M204-R02M-60 detector units. During operation, a reservoir on the detector was refilled with liquid nitrogen as per manufacturer instructions at least every seven hours. The cooling operation was necessary to keep the detector below a threshold temperature, above which detector performance was seriously degraded. The voltage signal from each detector was output to its own EE&G Judson PA-9 Transimpedance Preamplifier. Each preamplifier was powered by two Hewlett-Packard E3611A 12 volt, DC power supplies. The amplified signal from each detector was then output from its respective preamplifier to its assigned lock-in amplifier.

Lockin Amplifiers: Three lockin amplifiers were used in the experiment: one each for the detector output from each cell (Lockin One and Two for

Cells One and Two, respectively) and one for the output from the source detector (Lockin Three). All three lockin amplifiers were Stanford Research Systems model SR 510 Lockin Amplifiers. Each lockin also received the output of the chopper controller. The purpose of the lockin amplifiers was to accept the voltage output from the detectors, and using the frequency output from the chopper controller, screen out all of the intensity signals except those at the same frequency of the chopper. Thus, while the detectors might have been detected light signals from many light and infrared sources throughout the laboratory, only the light source associated with the experimental apparatus would have the same frequency as the chopper. Therefore, the voltage output of the lockin amplifiers represented the voltage output from the detectors created solely by the signal from the experimental light source incident upon the detectors.

Data Acquisition Board and Computer: A Intel 386SX based computer with an AT-MIO-16F-5 data acquisition board was used to acquire data from the voltage outputs of the three lockin amplifiers, the two thermocouples, and the two Baratron pressure transducers. A program was written in Microsoft Quick C to enable the Lab Windows data acquisition software to control the data acquisition board. The source code for the program is presented in Appendix A. The program was written such that the user could specify the data file title, the number of samples the data acquisition board would acquire, and the rate at which the board would take data samples. After experimental runs were completed, the data files created were transferred to a 486DX based computer for analysis using the Microsoft Excel and Table Curve software packages.

3.3.3 Procedure. The cross-section determination involved slowly

adding TCE vapor into the sample cells that had been previously evacuated, while continuously measuring the changes in light intensity measured by the detectors. The cells had been previously evacuated to remove any pressure interferences the presence of atmosphere might have caused. TCE vapor was then slowly added to the cells until the pressure in the cell reached the vapor pressure of TCE (58 torr at 20 °C). Next, the cells were slowly evacuated until vacuum was again achieved. As the TCE was added and evacuated from the sample cells, the cell temperature, cell pressure, and transmitted intensities were sampled by the data acquisition software at one second intervals. Using the data acquired, the TCE cross section was calculated (see Chapter 4).

3.4 Phase Three: Measuring TCE Desorption.

3.4.1 Purpose. The purpose of Phase Three was to measure the rate of TCE desorption over time from seven types of soil and to determine if any correlation existed between the rate and progress of desorption and the characteristics of the soil from which desorption is occurring. From these observations, increased understanding of the slow desorption mechanism and the affect soil characteristics have on that mechanism was to be gained.

In order to accomplish these measurements, the apparatus designed using the results from Phase One and assembled in Phase Two was used, and the cross-sectional area measurements from Phase Two were applied.

3.4.2 Equipment. The identical apparatus from Phase Two was used in accomplishing Phase.

3.4.3 Procedure. The description of the procedure performed in Phase Three has been divided into three sections: Sample Preparation, Apparatus Preparation, and Data Collection and Analysis.

3.4.3.1 Sample Preparation. The TCE desorption processes from seven types of soil (dolomitic limestone, flint clay, glass sand, Montana soil, plastic clay, San Joaquin soil, and sodium feldspar) were evaluated in Phase Three. A detailed listing of the characteristics of each soil type is included in Appendix B. A partial summary of the percent by weight elemental composition of each of the soils is presented in Table 2. Many of the soils included trace concentrations of many elements which were not included in the Table 2 summary or in subsequent data analysis.

Each sample was examined under a microscope at 50 times magnification to determine an average particle diameter. A slide with a thin film of soil grains was prepared and placed under the microscope. An average grain size determination was then performed by visual examination of the particle size distribution on the slide. This task was greatly aided by the high homogeneity of the soil samples. The diameter measurements for the samples are presented in Table 3. The diameters of the soils used in this research are not typical of soils found in the environment. For instance, natural clays have an average diameter of less than 2 μm. The highly processed clays procured for this research had diameters on the order 8-10 μm. This disparity was not considered a significant disadvantage, because the objective was to obtain soils with a variety of diameters to allow detailed analysis. Similarity to natural soils was a secondary objective. Extrapolation of the results to actual soils in the environment may still have validity when based strictly on diameter and elemental content.

TABLE 2

PERCENT BY WEIGHT ELEMENTAL COMPOSITION OF EXPERIMENT SOILS

Type	Al	Ca	Fe	K	Mg	Mn	Na	P	Si	S	T
Dolomite	0.34	29.95	0.28	0.10	21.03	0.02	0.03	0.04	1.13	0.00	0.00
Feldspar	20.50	2.14	0.07	5.20	0.02	0.00	6.20	0.02	65.20	0.00	0.01
Flint Clay	20.76	0.03	0.83	0.51	0.11	0.00	0.05	0.02	19.81	0.00	1.43
Glass Sand	0.66	0.00	0.08	0.00	0.00	0.00	0.00	0.00	95.00	0.00	0.12
Montana	6.44	1.25	3.38	2.11	0.85	1.01	1.14	0.11	28.97	0.24	0.28
Plastic Clay	14.30	0.08	1.18	2.81	0.36	0.01	0.15	0.03	26.65	0.00	0.81
San Joaquin	7.50	1.89	3.50	2.03	1.51	0.00	1.16	0.06	29.66	0.09	0.34

Adapted from National Institute of Standards and Technology Data, Appendix B.

TABLE 3

AVERAGE PARTICLE DIAMETER DATA FOR EXPERIMENT SOILS

Soil Type	Average Particle Diameter (μm)
Dolomitic Limestone	3
Flint Clay	8
Glass Sand	1
Montana Soil	2
Plastic Clay	10
San Joaquin Soil	5
Sodium Feldspar	8

Prior to initiation of an experimental run, a sample from the particular soil type to be tested was prepared. Two grams of each soil type were completely saturated with TCE liquid and placed in a sealed glass bottle for thirty-six hour period. Care was taken to ensure that the samples remained completely saturated throughout the thirty-six hour period. At the end of the contamination period, the seal was removed from the glass bottle and any remaining liquid TCE was allowed to evaporate. One of the soil samples, once dried through evaporation, was placed into one of the sample cells.

3.4.3.2 Apparatus Preparation. Prior to placement of the soil sample into a sample cell, the apparatus also was prepared. First, at least twelve hours prior to the start of an experimental run, the apparatus was evacuated, and for at least twelve hours a continuous vacuum was maintained on the system. Approximately 30 minutes prior to the initiation of a run, the InSb detectors were cooled with liquid

nitrogen, all equipment was activated, and the optical alignment of the detectors was verified. Next, to allow insertion of the soil sample into the sample cell, the vacuum pump was turned off and the ends of the cells were removed, exposing the cell to atmosphere. The soil sample was then spooned into the cell over an approximately ten minute period. Care was taken to ensure that any spilled soil was collected and reinserted into the cell.

3.4.3.3 Data Collection and Analysis. Upon completion of the soil insertion procedure, the ends of the cell were sealed and the cell was evacuated for sixty seconds to remove atmospheric interference. At the end of the sixty seconds, the valve to the vacuum pump was closed, data acquisition was initiated, and the TCE was allowed to begin to desorb within the sample cell. A sample of the transmitted intensity, cell temperature, and cell pressure was taken every sixty seconds over a thirty-six hour period. During the run time, the InSb detectors were refilled with liquid nitrogen at least every seven hours to maintain continuous operational capability.

During the run, the data being collected was monitored to ensure that the integrity of the apparatus had not failed. Also, the progress of the TCE desorption from the soil was closely monitored.

Due to the possibility of the cooling of the InSb detectors having an influence on their voltage output, care was taken to ensure that the detectors were cooled at least thirty minutes prior to any evacuation of the cell. This precaution was taken since the rate of desorption was expected to be most rapid immediately after the soil has been allowed to begin desorption.

At the end of the run, the sample cells were completely cleaned with acetone and cotton swabs and care was taken to ensure that no

pressure leaks were created during the cleaning procedure.

Due to the relatively long run times inherent in measuring the rate and progress of desorption in Phase Three compared to the much shorter run times in Phase Two, the behavior of the InSb detectors over time was investigated. Because the detectors must be refilled at least every seven hours with liquid nitrogen, there was a concern that over time there might be a slight degradation of detection ability up to complete failure at seven hours. To test this behavior, two preliminary runs of Phase Three was performed for each detector with no TCE or soil present in the cell and constant vacuum maintained on the cells throughout the run. Ideally, the intensity output from the detector would have remained constant throughout the run.

Unfortunately, a drift in detector response was measured. The drift followed a pattern of an initially fast decrease in intensity followed by a leveling off for the duration of the testing (up to 36 hours). The observed effect of the decreasing intensity gave the impression that there is an increasing concentration of TCE in the sample cell that was not occurring. A curve fit of the actual detector response for Detector 1 is shown in Figure 4. The curve fit for Detector 2 is shown in Figure 5.

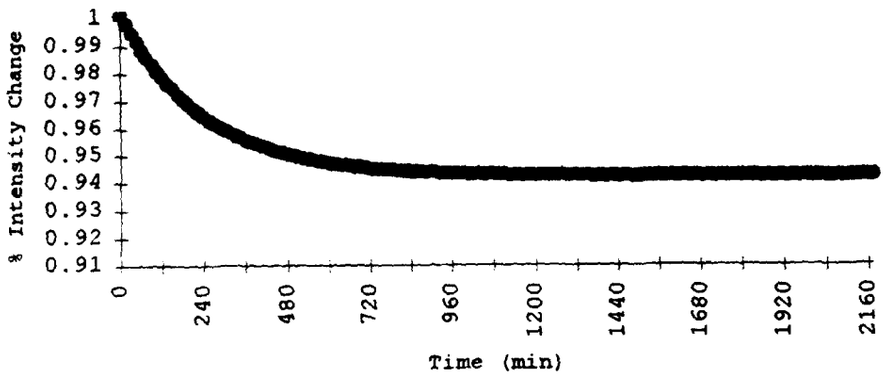

Figure 4. Curve Fit of Detector 1 Drift.

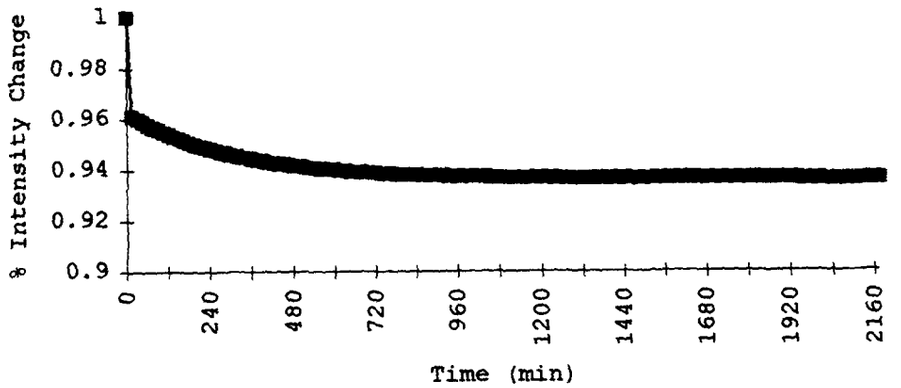

Figure 5. Curve Fit of Detector 2 Drift.

The following equations represent the curve fits determined for Detectors 1 and 2, respectively:

$$\frac{I_{exp}}{I_{empty}} = 0.9425 + 0.0593\, e^{-(\text{minutes}/239.78)} \qquad (18)$$

$$\frac{I_{exp}}{I_{empty}} = 0.9362 + 0.0264\, e^{-(minutes/300.33)} \quad (19)$$

Equations 45 and 46 provided the percent reduction to the measured intensity values as a function of time which represented the drift in detector performance. All data presented in Phase Three of this thesis has undergone the above detector drift correction.

After all seven desorption runs were complete, the data was compiled and a curve fit of the Langmuir Isotherm functional form (Equation 10) was performed with each data set. From these curve fits, values for the two Langmuir Isotherm parameters, μ and K_d, were determined for each soil type. In determining the value of μ, the parameter measuring the ultimate amount of TCE desorbed from the soil as time goes to infinity, the assumption was made that this value could be determined by using data collected over approximately 36 hours. Upon determination of μ and K_d values for each soil type, the correlation of these values were checked with respect to average soil particle diameter and elemental composition data. Correlation coefficient values equal to or greater than 0.50 were considered significant.

3.5 Limitations of the Research.

Due to the nature of the methodology chosen to study the desorption phenomena, certain limitations existed in the accuracy and precision of this research. The acknowledged limitations included:

1. The degree of microbial activity in the soil was not determined, measured, or controlled. However, the soil was kept in

sealed containers until approximately 36 hours prior to run initiation, at which time it was completely saturated with TCE. Additionally, the soil from the National Institute of Standards was highly processed, oven dried, and homogenized to ensure its purity.

2. The water content of the soil was not evaluated prior to collection of data. However, the sample cells were placed under vacuum, it was felt that any liquid or vapor phase water in the cells would be effectively evacuated prior to data collection.

3. The pressure leak rates between the two sample cells may not have been identical. However, small leaks in pressure (1 torr over 24 hours) should not have had a significant effect on the concentration of TCE within the cells and hence the data collection performed.

4. In designing the experiment apparatus, care was taken to choose materials that would not significantly absorb TCE. However, if such absorption did occur, interpretation of the data collected in this thesis could be problematic. However, control runs with no soil present in the sample cell and with the apparatus exposed to TCE were performed and no effects of apparatus absorption/desorption were detected.

5. Although spectroscopic grade laboratory TCE was used in this research, no additional control was maintained over TCE quality and purity. Potential additives in the TCE may have had a small affect on its desorption characteristics and performance.

6. At the beginning of each experiment run, after the soil was placed in the sample cells, but before data collection was initiated,

the cells were evacuated for approximately 30 seconds to remove atmosphere. During this initial evacuation, any remaining liquid-phase, non-adsorbed TCE was also to be evacuated. Almost certainly, during this 30 second vacuum period some adsorbed TCE was also removed. The removal of this TCE may have had an affect on the subsequent rate and progress of the desorption of the remaining TCE.

IV. Results

4.1 Phase One.

Low-resolution (4 cm^{-1}) scans of a sample containing TCE vapor indicated a promising absorption feature in the vicinity of 3100 cm^{-1} wave numbers. A plot of the low resolution scan (percent transmittance versus wave number) is included in Figure 6.

A high resolution (0.02 cm-1) scan of the TCE vapor sample confirmed that TCE readily absorbs electromagnetic energy between 3050 cm^{-1} and 3130 cm^{-1} in frequency. A plot of the high resolution scan is included in Figure 7. Inspection of reported water vapor and atmosphere absorption characteristics indicated that neither substance significantly absorbed electromagnetic energy in this region.

Using the high resolution scan data, design of a narrow bandpass filters for the Phases Two and Three sample cells was performed. The filters were specified such that only a frequency range of 3040 - 3140 cm^{-1} would be transmitted. The band pass range of the filters exceeded the adsorption range of the TCE vapor by 10 cm^{-1} wave numbers on either side as required in the design criteria discussed in Chapter Three. A high resolution scan of the filter is included in Figure 8.

Figure 6. Low Resolution Scan of TCE Absorbtion

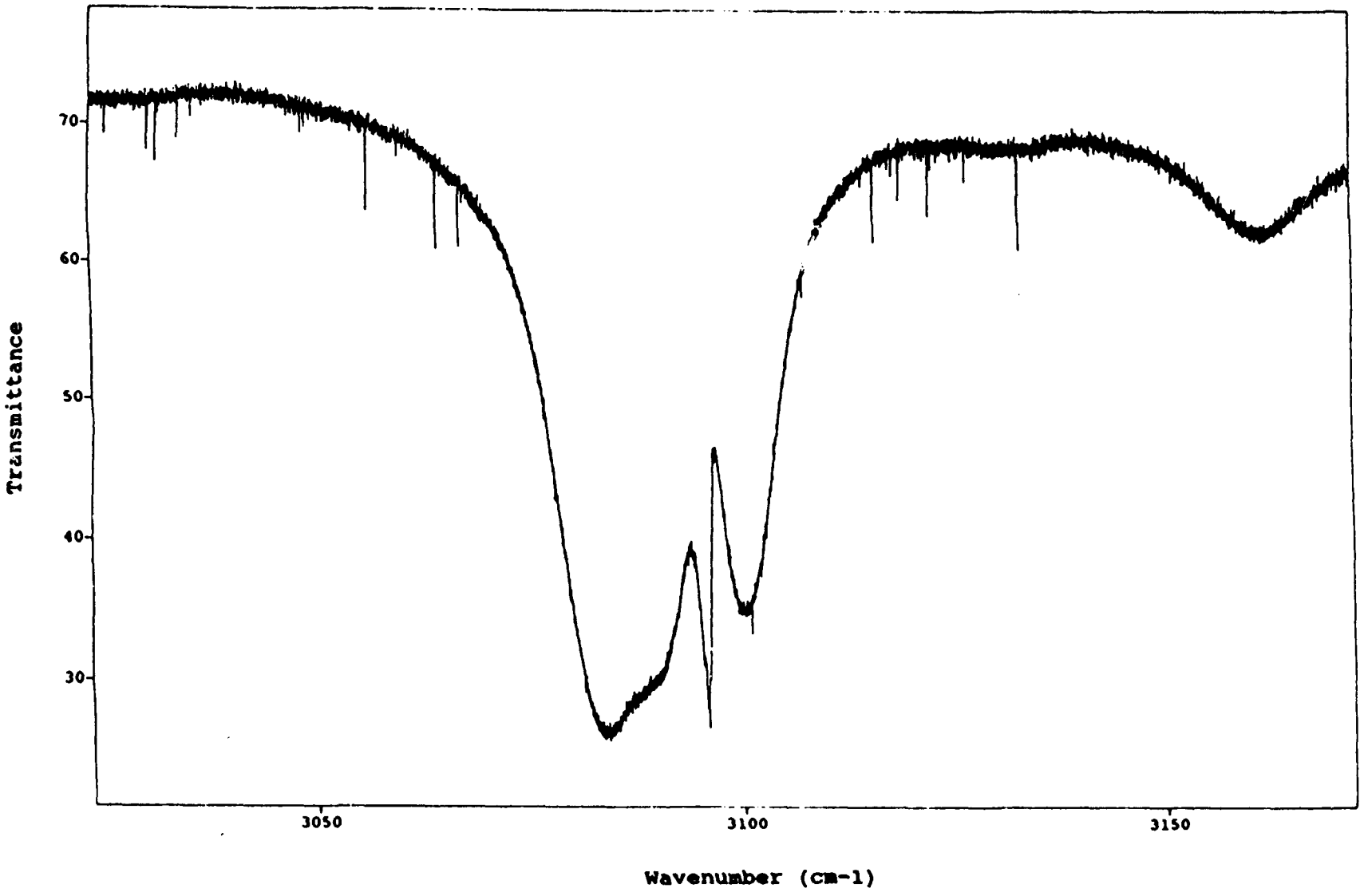

Figure 7. High Resolution Scan of TCE Absorbtion

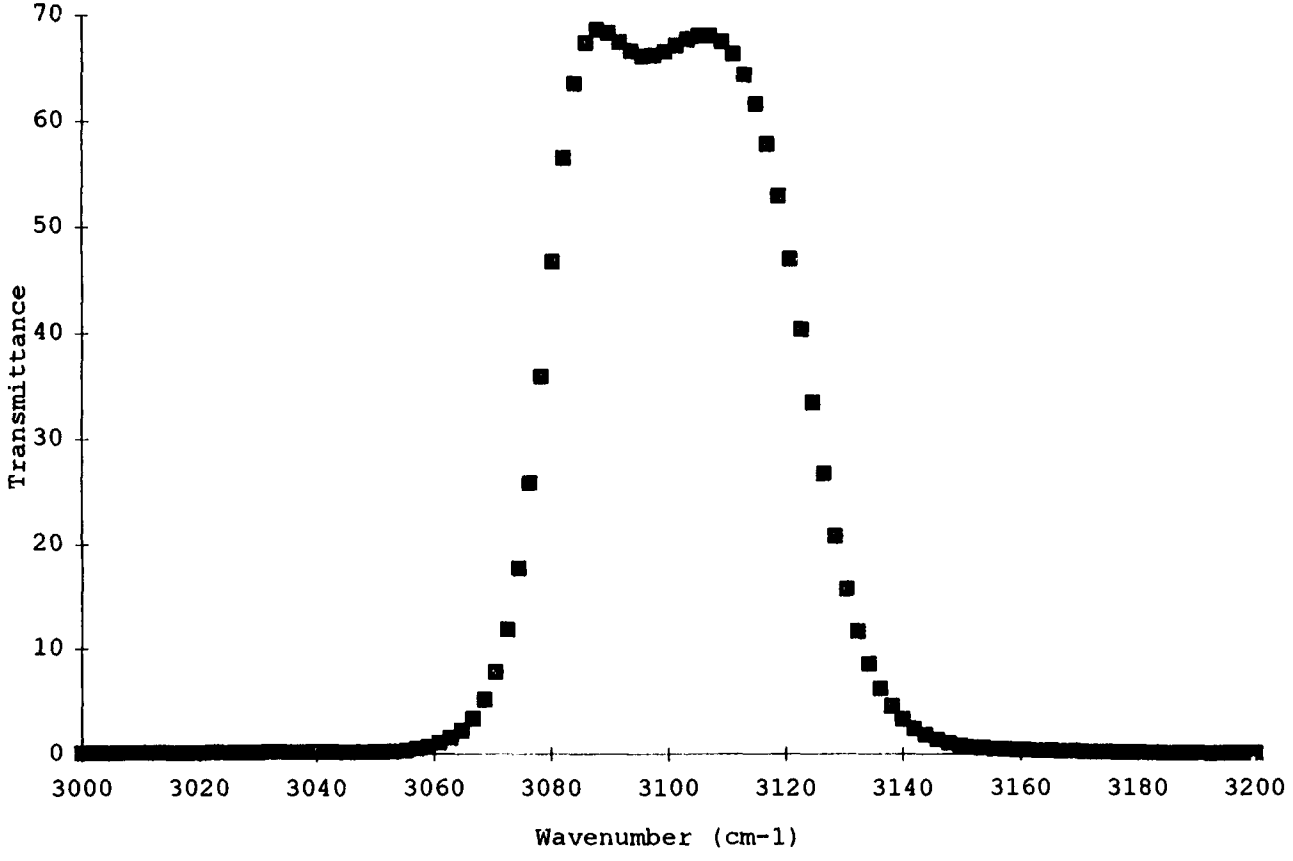

Figure 8. High Resolution Scan of Bandpass Filter

4.2 Phase Two.

Using the experimentally gathered pressure and intensity data, the optical absorption cross-sectional area, σ, for vapor-phase TCE molecules was calculated. Solving for σ using the pressure and intensity data gathered required the use of Beer's Law (Equation 16) and the Ideal Gas Law (Serway, 1983: 686). The Ideal Gas Law may be stated as follows:

$$PV = n R T \tag{20}$$

where:

P = Pressure (torr) within the cell.

V = Volume (cm^3) of the cell.

n = Number of molecules within the cell.

R = Gas Constant.

$$= 0.0821 \ \frac{lit - atm}{mol - {}^{o}K}.$$

$$= 1.0356 \times 10\text{-}19 \ \frac{cm^3 - torr}{mol - {}^{o}K}.$$

T = Temperature with the cell (°K); maintained at a constant 300 °K throughout Phase Two experiment.

The Ideal Gas Law was used to calculate the concentration of TCE $\left(\frac{molecule}{volume}\right)$ within the cell. As described in Chapter 3, pressure conditions within the cell were changed from vacuum to approximately 58 torr (the vapor pressure of TCE at 20 °C) and then back to vacuum by adding and then evacuating TCE vapor slowly from the cell. As conditions in the cell varied, cell pressure and transmitted intensity

data were gathered at one second intervals, providing the necessary inputs for the Ideal Gas Law to calculate the concentration of TCE within the cell. Rearranging Equation 20 for this operation yielded:

$$N = \frac{n}{V} = \frac{P}{RT} \tag{21}$$

where:

N = The concentration of TCE within the cell $\left(\frac{\text{molecules}}{\text{cm}^3}\right)$.

Using the calculated TCE concentration values, Beer's Law was used to solve for the only remaining variable in the equation, σ. To apply the results of Equation 21 to solve for σ, Equation 16 was therefore rearranged as follows:

$$\sigma = - \frac{\ln\left(\frac{I_t}{I_o}\right)}{l\ N} \tag{22}$$

Equation 21 was then substituted into Equation 22. The following equation for σ resulted:

$$\sigma = - \frac{\ln\left(\frac{I_t}{I_o}\right) R\ T}{P\ l} \tag{23}$$

Prior to analyzing the data obtained in Phase Two, the basic assumption was made that the optical cross-section of TCE would be constant at a constant temperature. In conducting Phase Two, the temperature (300 °K) and the path length (43.5 cm) were also held

constant. Therefore, inspection of Equation 23 indicated that a plot of pressure versus $\ln\left(\frac{I}{I_o}\right)$ would be expected to be linear with a negative slope, as follows:

$$P = - \frac{R\,T}{l\,\sigma} \ln\left(\frac{I}{I_o}\right) \tag{24}$$

Hence, when pressure data was plotted versus the $\ln\left(\frac{I}{I_o}\right)$ data, the slope of the line would be $\left(- \frac{R\,T}{l\,\sigma}\right)$. Consequently, σ was to be determined by measuring the slope of pressure versus $\ln\left(\frac{I}{I_o}\right)$ and solving for σ.

Unfortunately, the pressure versus $\ln\left(\frac{I}{I_o}\right)$ plot did not depict a linear relationship. This graph is shown in Figure 9. As shown in the graph, the actual plot did not have the constant slope as was predicted by Equation 24.

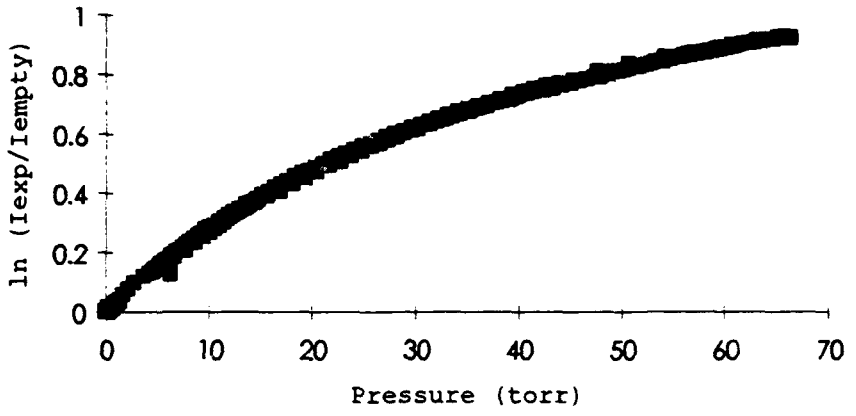

Figure 9. Uncorrected Cross-Sectional Area Plot

As was explained in Chapter 3, the optical filter designed in Phase One allowed a frequency range of light to pass that not only encompassed, but also exceeded the range of the TCE absorption feature selected for study. Therefore, regardless of how high the concentration of TCE vapor was within a sample cell, there always would be a component of the unabsorbed signal that the filter would allow to pass to the detector. To accurately measure the cross-sectional area of TCE molecules and, subsequently, the concentration of TCE within the sample cells, this unaffected intensity component had to be accounted for in the data.

In order to derive a correction to experimental data, the relationship between the absorption spectrum of TCE and the transmittance of the bandpass filters was analyzed. Inspection of the optical path of the experimental apparatus indicated that the signal transmitted from the light source passed through the sample cell containing TCE vapor and through the bandpass filter before reaching the face of the InSb detector. Therefore, the intensity measured by the detector was as follows:

$$I_{exp}(\nu) = I_o\, T(\nu)\, e^{-\sigma(\nu)\, l\, N} \qquad (25)$$

where:

$I_{exp}(\nu)$ = The experimental intensity measured by the detector after the signal has been transmitted through the sample cell and the bandpass filter.

I_o = The intensity signal transmitted by the light source, independent of any effects from TCE absorption or bandpass filter blockage; assumed to be constant.

$T(\nu)$ = The intensity allowed to pass through the bandpass filter as a function of frequency, υ.

$e^{-\sigma(\nu)\, l\, N}$ = The signal intensity as a function of frequency after being transmitted through a sample of TCE (according to Beer's law).

Equation 25 was then evaluated over the range of frequencies visible to the detector (effectively 0 to ∞ wavenumbers), as follows:

$$\int_0^\infty I_{exp}(\nu)\, d\nu = \int_0^\infty I_o\, T(\nu)\, e^{-\sigma(\nu)\, l\, N}\, d\nu \qquad (26)$$

Next, Equation 26 was evaluated for the case in which no TCE was present in the sample cell. In this case, the concentration of TCE, N, was zero, and the following equation resulted:

$$\int_0^\infty I_{Empty}(\nu)\, d\nu = \int_0^\infty I_o\, T(\nu)\, d\nu \qquad (27)$$

where:

$I_{Empty}(\nu)$ = The intensity measured by the detector as a function of frequency when the sample cell is evacuated

Evaluating the ratio of $I_{exp}(\nu)$ to $I_{Empty}(\nu)$ resulted in the following equation:

$$\frac{I_{exp}}{I_{Empty}} = \frac{\int_0^\infty T(\nu)\, e^{-\sigma(\nu)\, l\, N}\, d\nu}{\int_0^\infty T(\nu)\, d\nu} \qquad (28)$$

To simplify the integration of Equation 28, rectangular approximations of the area under the curves of the transmission spectrum of TCE and the filter were conceived. The filter transmission spectrum (Figure 8) was evaluated using a Bio-Rad Fourier Transform Infrared Spectrometer, Model 60A, and the TCE absorption spectrum was evaluated using the high resolution scan obtained in Phase One.

Three figures depict the rectangular approximation of the transmission curves of TCE (Figure 10), the bandpass filter (Figure 11), and the combined apparatus (Figure 12). Each of the figures show a plot of signal frequency versus the fraction the signal that is transmitted. In Figure 10, the shaded area represents the portion of the signal that is not absorbed by the TCE in the sample cell. In Figure 11, the shaded area represents the portion of the signal that is not blocked by the

bandpass filter. Finally, in Figure 12, the shaded area, Region 4, represents the area affected neither by the TCE nor the filter, and transmitted to the face of the detector. Region 1 indicates the portion of the signal blocked by the filter. Region 3 indicates the portion blocked by TCE absorption. Region 2 indicates the portion blocked by both the filter and TCE absorption.

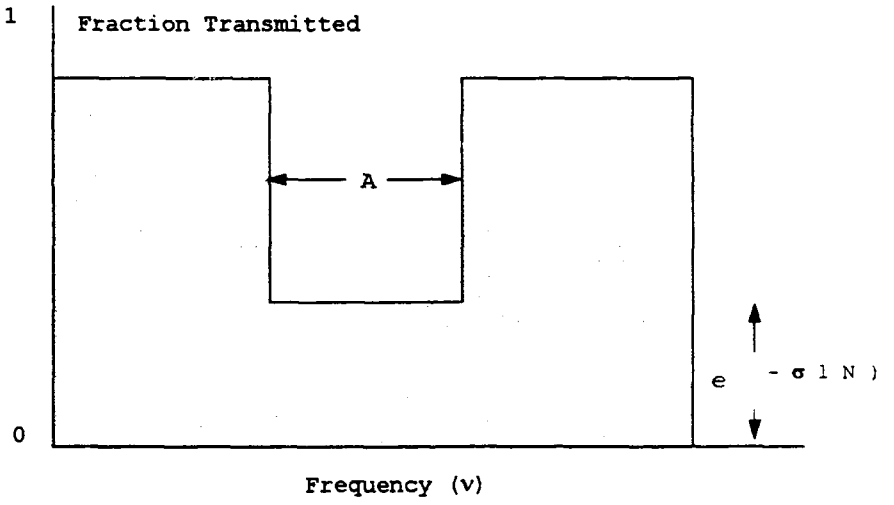

Figure 10. Rectangular Approximation of TCE Transmission

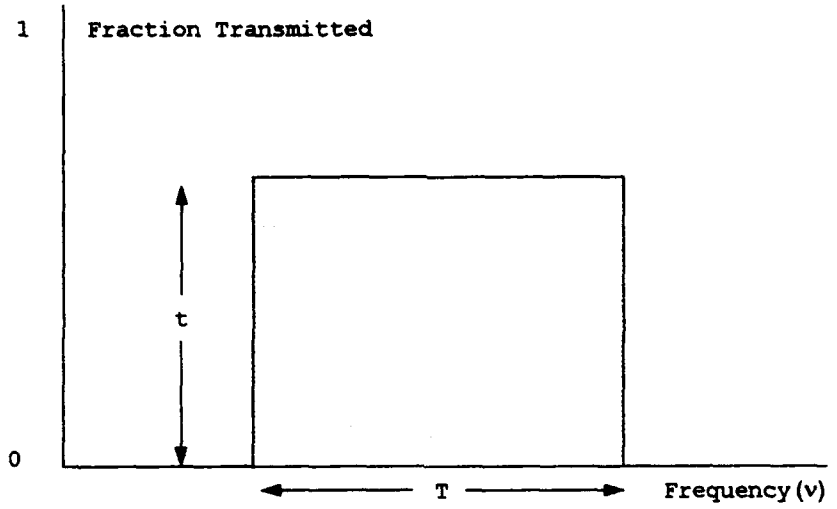

Figure 11. Rectangular Approximation of Bandpass Filter Transmission

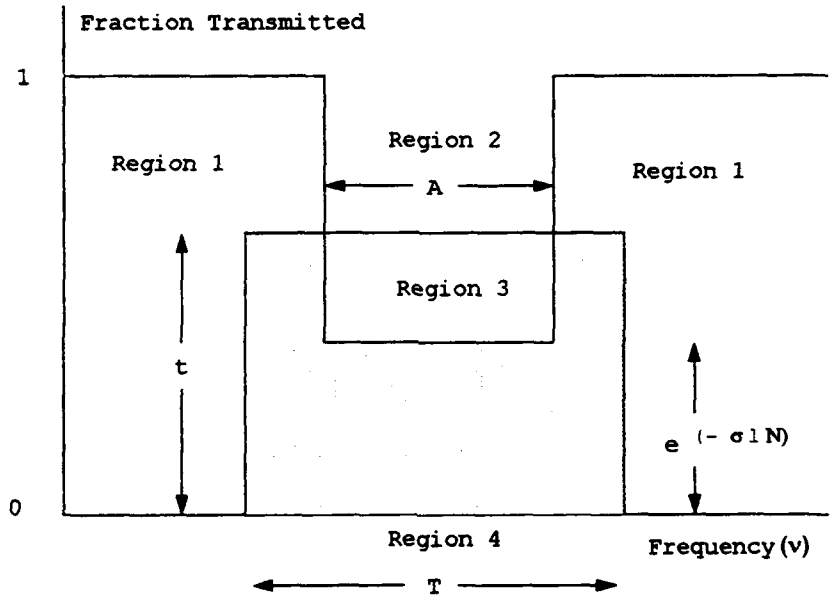

Figure 12. Rectangular Approximation of Experiment Apparatus

Applying the rectangular approximations to Equation 20 resulted in the following equation:

$$\frac{I_{exp}}{I_{empty}} = \frac{t(T-A) + (A)(t)e^{-\sigma l N}}{Tt} \quad (29)$$

or

$$\frac{I_{exp}}{I_{empty}} = \left[1 - \frac{A}{T}\right] + \frac{A}{T} e^{-\sigma l n} \quad (30)$$

Rearranging Beer's Law, Equation 16, provided the relation:

$$\frac{I_t}{I_o} = e^{-\sigma l N} \quad (31)$$

where:

$\frac{I_t}{I_o}$ = The fraction of the source's intensity output incident upon the detector, decayed solely through TCE absorption (no filter effects).

Substituting Equation 31 into Equation 30 resulted the following equation:

$$\frac{I_t}{I_o} = \frac{T}{A} * \left[\frac{I_{exp}}{I_{empty}} - \left(1 - \frac{A}{T} \right) \right] \quad (32)$$

Thus, using the experimentally gathered intensity data, the amount of signal degradation caused by TCE absorption alone was able to be calculated. Examination of the high resolution scans of TCE and the bandpass filter (Figures 7 and 9, respectively) provided approximated values for T and A as follows:

$$T = 43\ cm^{-1} \tag{33}$$

$$A = 29\ cm^{-1} \tag{34}$$

Applying these values to Equation 32 resulted in:

$$\frac{I_t}{I_o} = \frac{43}{29} * \left[\frac{I_{exp}}{I_{empty}} - \left(1 - \frac{29}{43} \right) \right] \tag{35}$$

and solving resulted in:

$$\frac{I_t}{I_o} = 1.5 * \left[\frac{I_{exp}}{I_{empty}} - 0.33 \right] \tag{36}$$

Applying Equation 36 to the experimental data yielded the desired correction to enable determination of the cross-sectional area. A plot of the corrected data is shown in Figure 13. The slope of this curve was calculated to be -0.04755 using a linear regression fit. Applying this value to Equation 23 allowed calculation of the cross-section as follows:

$$\sigma = -(-0.04755) * \frac{(1.036\ E-19)\ \ (300\ ^{\circ}K)}{43.5\ cm} \tag{37}$$

Solving this equation resulted in:

$$\sigma = 3.27E\text{-}20 \text{ cm}^2/\text{molecule} \tag{38}$$

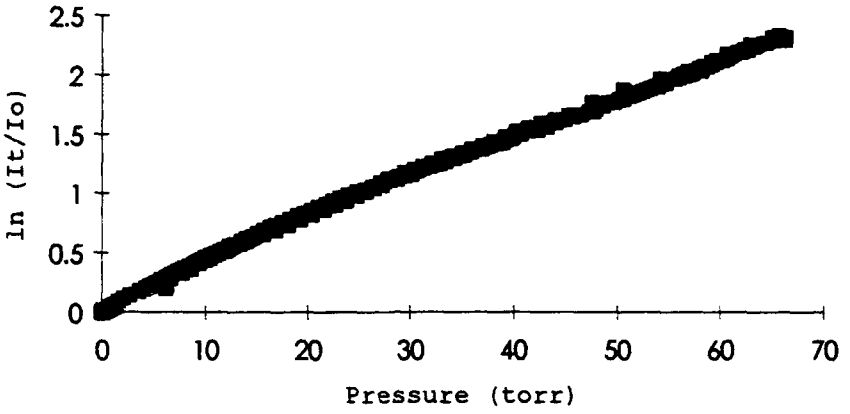

Figure 13. Corrected Cross-Sectional Area Plot

To ensure the most accurate fit to the Phase Two data when calculating the cross-sectional area, the software package Table Curve was also used. To apply the program to the experimental data required combining Equations 23 and 32 as follows:

$$\sigma = -\frac{\ln \frac{T}{A}\left[\frac{I_{exp}}{I_{empty}} - \left[1 - \frac{A}{T}\right]\right]}{P} * \frac{R\,T}{l} \tag{38}$$

To simplify this equation, the following terms were defined:

$$Y = \frac{I_{exp}}{I_{empty}}$$

$$X = P$$

$$B = -\frac{\sigma\, l}{T\, R}$$

$$C = \frac{A}{T}$$

Substitution these values into Equation 38 resulted in the following functional form:

$$Y = C\, e^{-Bx} + (1 - C) \qquad (39)$$

This functional form was evaluated using the $\frac{I_{exp}}{I_{empty}}$ and pressure data obtained during the Phase Two runs. Using Table Curve, the best fit values for variables B and C were determined. The values determined for each cell were as follows:

Cell	B	C	R-Squared
Cell 1	0.0464	0.638	0.995
Cell 2	0.0469	0.623	0.996

Applying these values to the above terms and solving for the cross-sectional area resulted in the following expressions for Cell 1:

$$\sigma = 3.32\text{E-}20 \text{ cm}^2\text{/molecule} \qquad (40)$$

and

$$\frac{I_t}{I_o} = \left[\frac{I_{exp}}{I_{empty}} - 0.36 \right] * 1.57 \qquad (41)$$

For Cell 2 the calculations resulted in:

$$\sigma = 3.35E\text{-}20 \text{ cm}^2/\text{molecule} \qquad (42)$$

and

$$\frac{I_t}{I_o} = \left[\frac{I_{exp}}{I_{empty}} - 0.38 \right] * 1.61 \qquad (43)$$

Due to the greater precision allowed in the calculation of the cross-sectional area using Table Curve, Equations 41 and 43 were felt to be representative of the experimental data. Because of the cross-sectional area values for the two cells differed by only 3E-22 cm^2/molecule, an average of the two cell values was selected for use in Phase Three. This resulted in the following final corrected cross-section values:

$$\sigma = 3.335E\text{-}20 \qquad (44)$$

$$\frac{I_t}{I_o} = \left[\frac{I_{exp}}{I_{empty}} - 0.37 \right] * 1.59 \qquad (45)$$

4.3 Phase Three.

Phase Three involved the measurement of the desorption of TCE from

seven types of soil. Measuring the desorption process involved the measurement of the concentration of TCE vapor within the sample cells over time. To measure changes in the TCE concentration within a cell, voltage readings from the output of the InSb detector were taken and corrected using Equation 45. To facilitate later interpretation of the results of Phase Three, the voltage data was converted to values of concentration (molecules/cm^3).

To accomplish the voltage to concentration conversion, Beer's Law, Equation 16, was rearranged as follows:

$$N = - \frac{\ln \frac{I_t}{I_o}}{\sigma l} \tag{46}$$

Applying Equation 46 and substituting in Equation 45 yield the corrected TCE concentrations in molecules/cm^3:

$$N = - \frac{\ln\left[\left[\frac{I_{exp}}{I_{empty}} - 0.37\right] * 1.59\right]}{\sigma l} \tag{47}$$

substituting the values obtained in Phase Two resulted in:

$$N = - \frac{\ln\left[\left(\frac{I_{exp}}{I_{empty}} - 0.37\right) * 1.59\right]}{(3.335E-20 \ \frac{cm^2}{molecule})\ (43.5\ cm)} \tag{48}$$

Solving Equation 48 resulted in the concentration determination equation:

$$N = (-6.89E17) * \ln\left[\left(\frac{I_{exp}}{I_{empty}} - 0.37\right) * 1.59\right] \quad (49)$$

During the operation of the Phase Three runs, it was useful to compare the intensity data being collected to the pressure within sample cell. As the concentration of TCE in the cell increased, the transmitted light intensity was expected to decrease (increased absorption by an increased number of TCE molecules) and the pressure in the cell was expected to increase. To enable comparison of the changes in intensity to the changes in pressure, a conversion equation was derived.

First, the Ideal Gas Law, Equation 21, was substituted into Equation 49 as follows:

$$P_i = -0.0714 * T * \ln\left[\left(\frac{I_{exp}}{I_{empty}} - 0.37\right) * 1.59\right] \quad (50)$$

where:

P_i = Pressure computed from intensity data.

Equation 50 related the voltage output from the InSb detectors to the pressure in the cell caused by the measured concentration of TCE vapor. This data was compared to the measured pressure in the cell throughout the Phase Three runs as a check to ensure the device was running properly. Changes in the pressure measurements that did not coincide with changes in intensity, or vice versa, were an indication of a severe pressure leak or some other failure in the experiment operation.

Throughout the runs, care was taken to ensure that all data presented in the thesis document were free of such errors.

The seven runs of Phase Three resulted in seven plots of TCE concentration versus time. The plots of the data are presented in the following figures: dolomitic limestone (Figure 14), flint clay (Figure 15), glass sand (Figure 16), [illegible] soil (Figure 17), plastic clay (Figure 18), San Joaquin soil (Figure 19), and sodium feldspar (Figure 20).

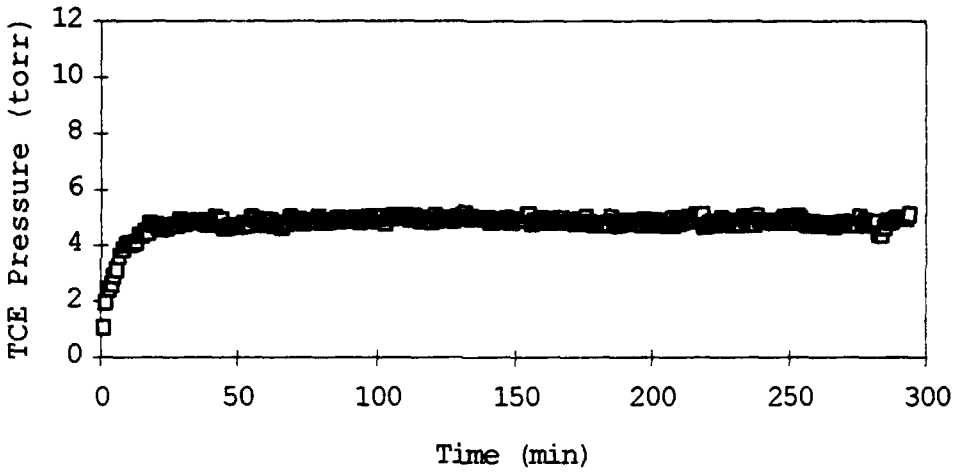

Figure 14. Desorption of TCE from Dolomitic Limestone

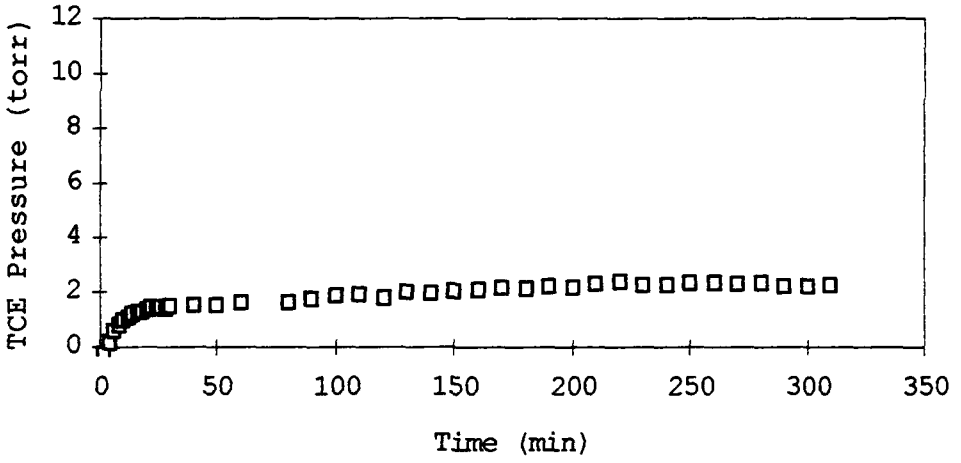

Figure 15. Desorption of TCE from Flint Clay

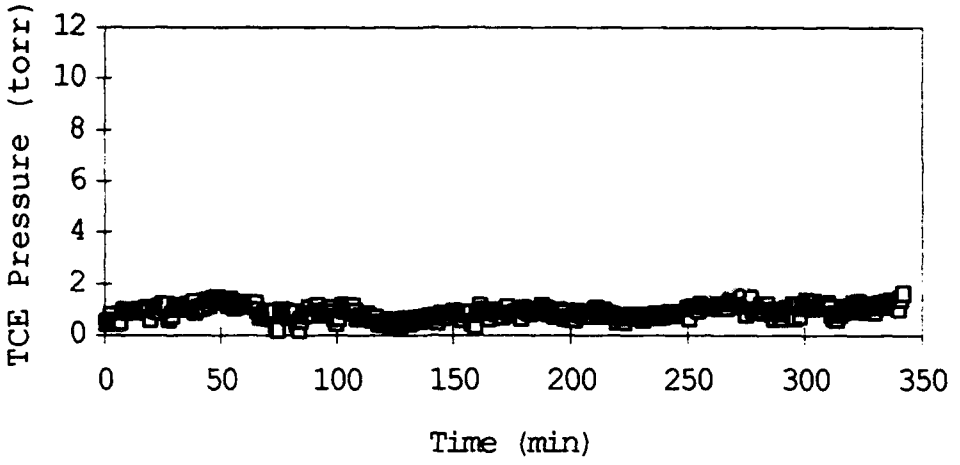

Figure 16. Desorption of TCE from Glass Sand

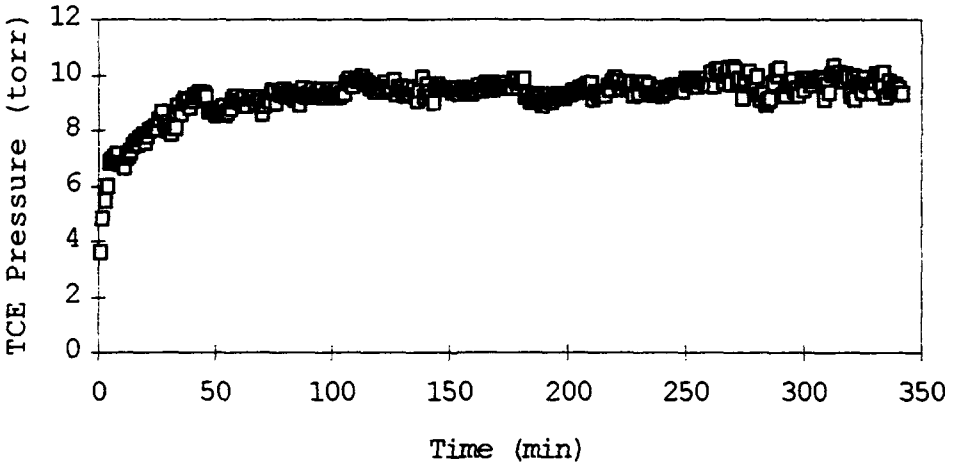

Figure 17. Desorption of TCE from Montana Soil

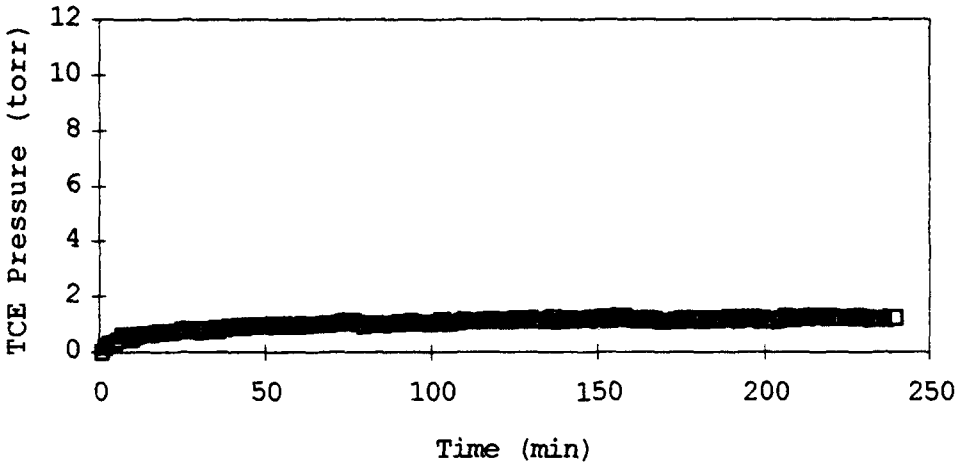

Figure 18. Desorption of TCE from Plastic Clay

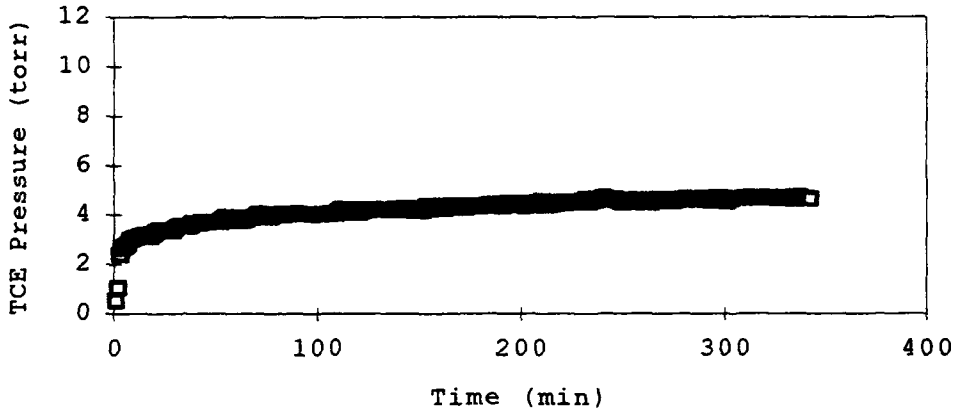

Figure 19. Desorption of TCE from San Joaquin Soil

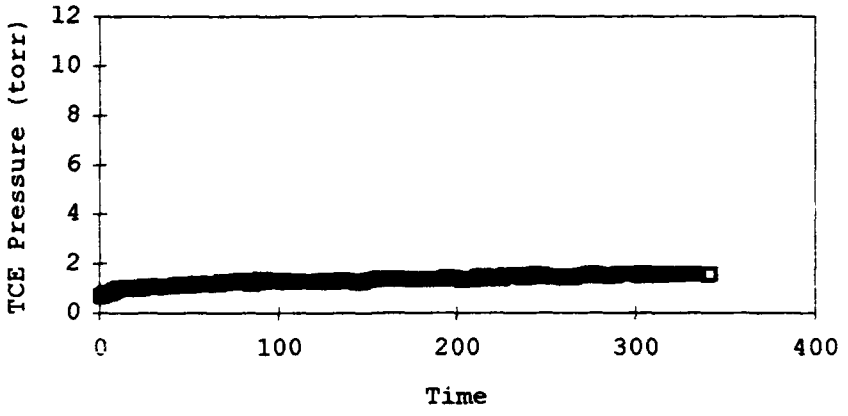

Figure 20. Desorption of TCE from Sodium Feldspar

Each of the seven data sets were analyzed using the Langmuir Isotherm model presented in Chapter 2, Equation 10. The assumptions made in Chapter 2 that the reabsorption of TCE into the soil would be negligible and that all of the available sorption sites on the soil were initially occupied were maintained in the analysis of the Phase Three data. Thus, the desorption model applied to the data was as follows:

$$TCE\ (t) = \mu\ (1 - e^{-\frac{K_d}{\mu}\ t}) \qquad (10)$$

The Table Curve software package was applied to determine the best fit of the functional form of Equation 10 to the data and to determine the μ and K_d parameters for each soil type. The parameters determined for each soil type along with the correlation coefficients for the curve fits are listed in Table 4.

TABLE 4

μ AND K_d VALUES CALCULATED USING LANGMUIR ISOTHERM FUNCTIONAL FORM

Soil Type	μ (mol/cm^3)	μ Standard Error	K_d (mol/cm^{3}sec)	K_d Standard Error	R^2
Dolomitic Limestone	4.8502	0.003865	0.8944	0.007989	0.9186
Flint Clay	2.1161	0.003810	0.0948	0.006761	0.8870
Glass Sand	0.9141	0.081893	0.2594	0.082994	0.0287
San Joaquin Soil	4.3316	0.003713	0.3517	0.019703	0.5901
Plastic Clay	1.1692	0.001175	0.0440	0.006761	0.8652
Montana Soil	9.4013	0.006329	1.3989	0.029127	0.5858
Sodium Feldspar	1.3811	0.003353	0.0849	0.009151	0.3916

Plots of the Langmuir Isotherm functional form curve fit to the data were prepared and presented in the following figures: dolomitic limestone (Figure 21), flint clay (Figure 22), glass sand (Figure 23), Montana soil (Figure 24), plastic clay (Figure 25), San Joaquin soil (Figure 26), and sodium feldspar (Figure 27).

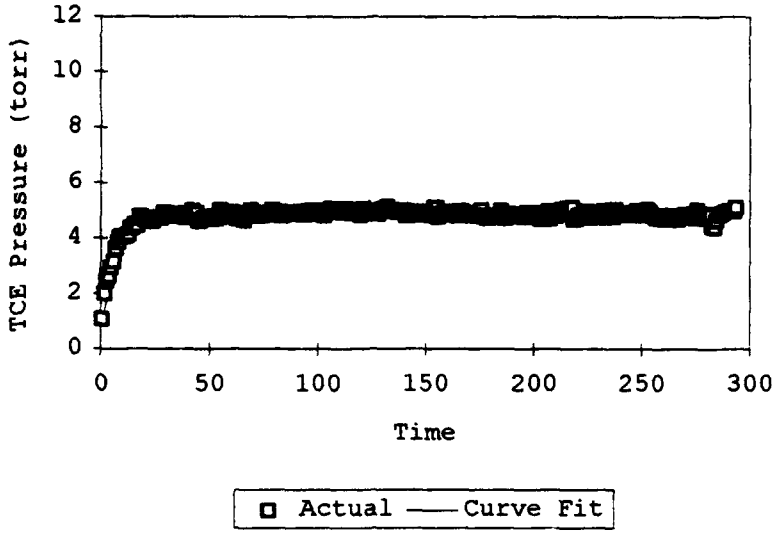

Figure 21. Curve Fit of Langmuir Isotherm Functional Form to TCE Desorption from Dolomitic Limestone Data.

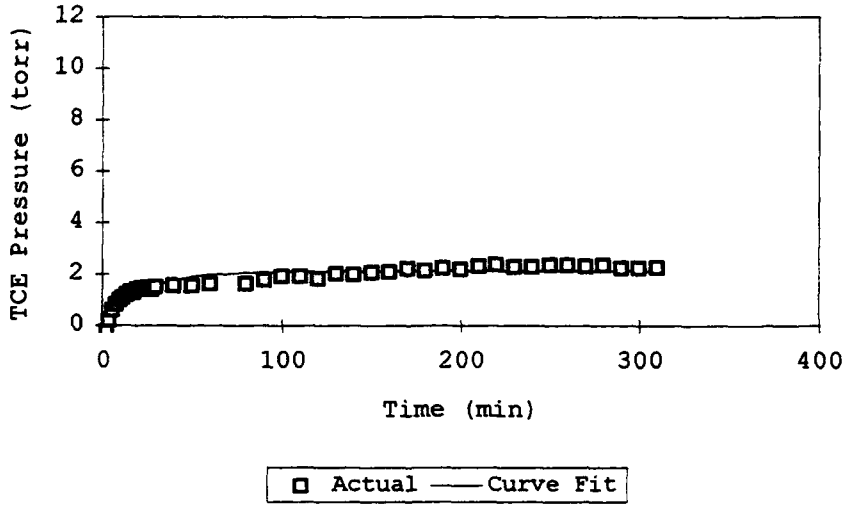

Figure 22. Curve Fit of Langmuir Isotherm Functional Form to TCE Desorption from Flint Clay Data.

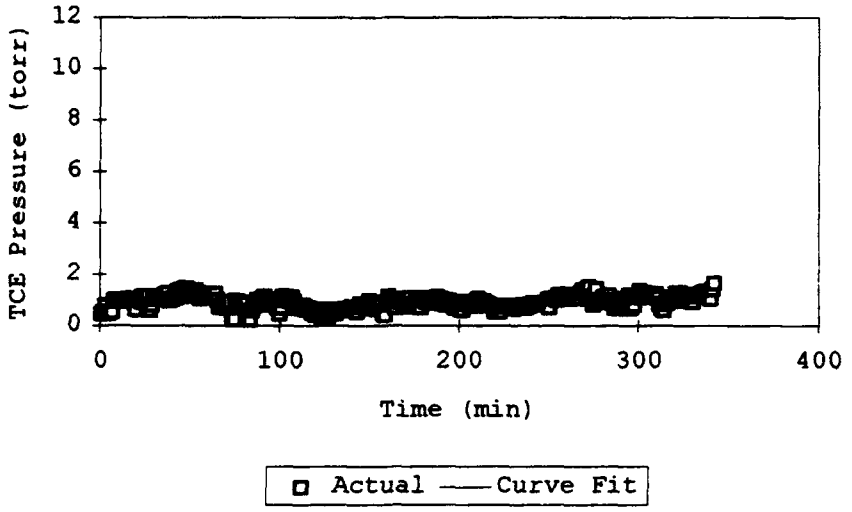

Figure 23. Curve Fit of Langmuir Isotherm Functional Form to TCE Desorption from Glass Sand Data.

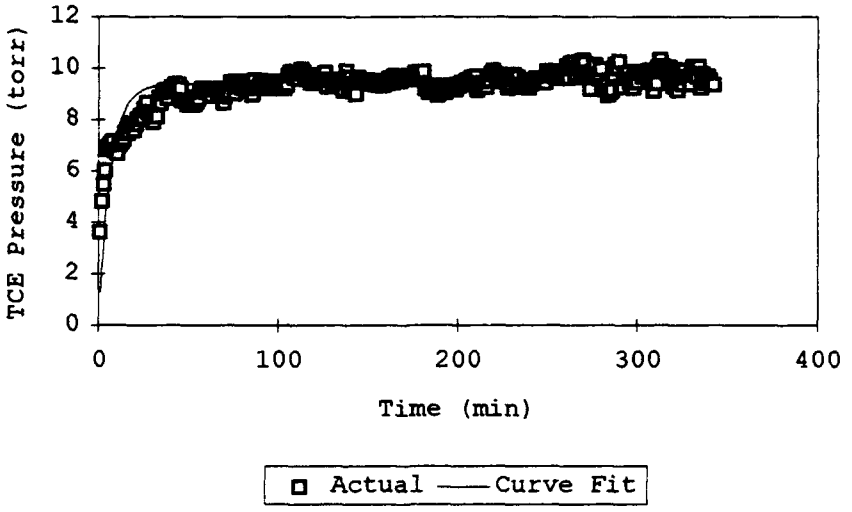

Figure 24. Curve Fit of Langmuir Isotherm Functional Form to TCE Desorption from Montana Soil Data.

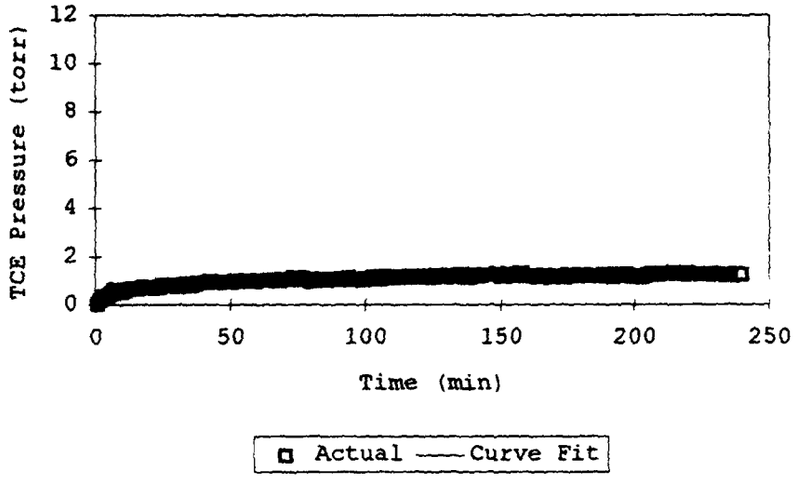

Figure 25. Curve Fit of Langmuir Isotherm Functional Form to TCE Desorption from Plastic Clay Data.

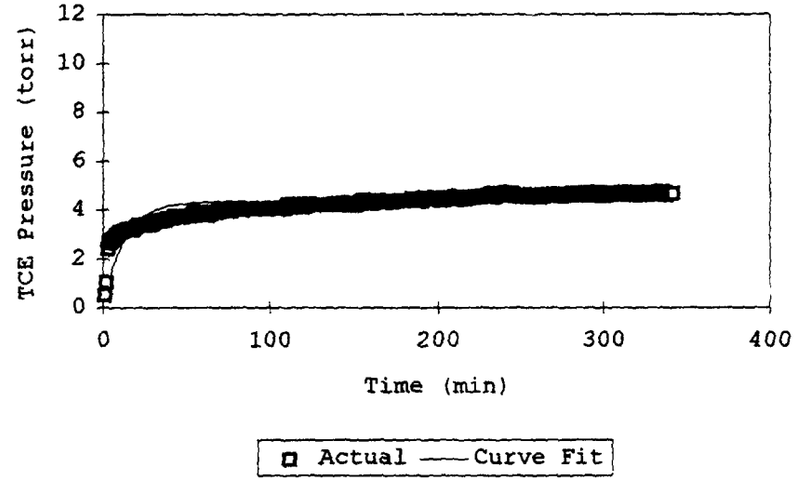

Figure 26. Curve Fit of Langmuir Isotherm Functional Form to TCE Desorption from San Joaquin Soil Data.

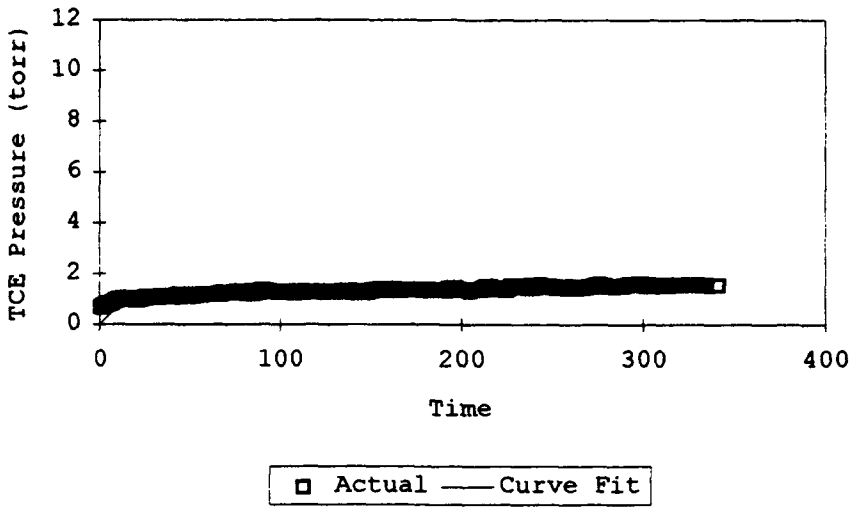

Figure 27. Curve Fit of Langmuir Isotherm Functional Form to TCE Desorption from Sodium Feldspar Data.

Curve fits of the Langmuir Isotherm with a coefficient of correlation of less than 0.5 were considered to be not representative of the data and were discarded from further analysis. Thus, the parameters calculated for glass sand and sodium feldspar were not used in the analysis of the desorption phenomena.

Curve fits with a correlation coefficient of greater than 0.5 were further analyzed in an effort to determine soil characteristics that influenced the calculated μ and K_d values. First, the average particle size diameters of the soils were compared to their associated μ and K_d values to determine in a correlation existed. Next, the percent by weight elemental composition of the soils was compared to their associated μ and K_d values to again check for a correlation. The coefficients of correlation for the soil characteristics with respect to μ and K_d are listed below in Table 5.

TABLE 5

CORRELATION OF SOIL CHARACTERISTICS WITH LANGMUIR ISOTHERM PARAMETERS

Soil Characteristic	Correlation with Kd	Correlation with Mu
Particle Diameter	-0.92	-0.90
Element		
Al	-0.71	-0.60
Ca	0.35	0.12
Fe	0.35	0.59
K	-0.11	0.03
Mg	0.34	0.11
Mn	0.82	0.88
Na	0.46	0.68
P	0.85	0.95
S	0.76	0.90
Si	-0.15	0.10
T	-0.70	-0.62

The characteristics that had positive or negative coefficients of correlation greater than 0.5 with K_d were considered significant influences on the desorption rate. These characteristics are listed below in Table 6.

TABLE 6

CHARACTERISTICS SHOWING SIGNIFICANT CORRELATION WITH K_d

Characteristic	Correlation with Kd
Particle Diameter	-0.89
Element	
Al	-0.89
Ca	0.76
Mg	0.75
P	0.56
Si	-0.56
T	-0.83

The characteristics that had positive or negative coefficients of correlation greater than 0.5 with μ were considered significant influences on the ultimate progress of desorption. These characteristics are listed below in Table 7. Plots of selected characteristics with significant correlation with K_d and μ are shown in Figures 28 (particle diameter versus K_d), 29 (particle diameter versus μ), 30 (percent by weight phosphorous content versus K_d), and 31 (percent by weight phosphorous content versus μ).

TABLE 7

CHARACTERISTICS SHOWING SIGNIFICANT CORRELATION WITH μ

Characteristic	Correlation with Mu
Particle Diameter	-0.67
Element	
Al	-0.60
Fe	0.59
Mn	0.88
Na	0.68
P	0.95
S	0.90

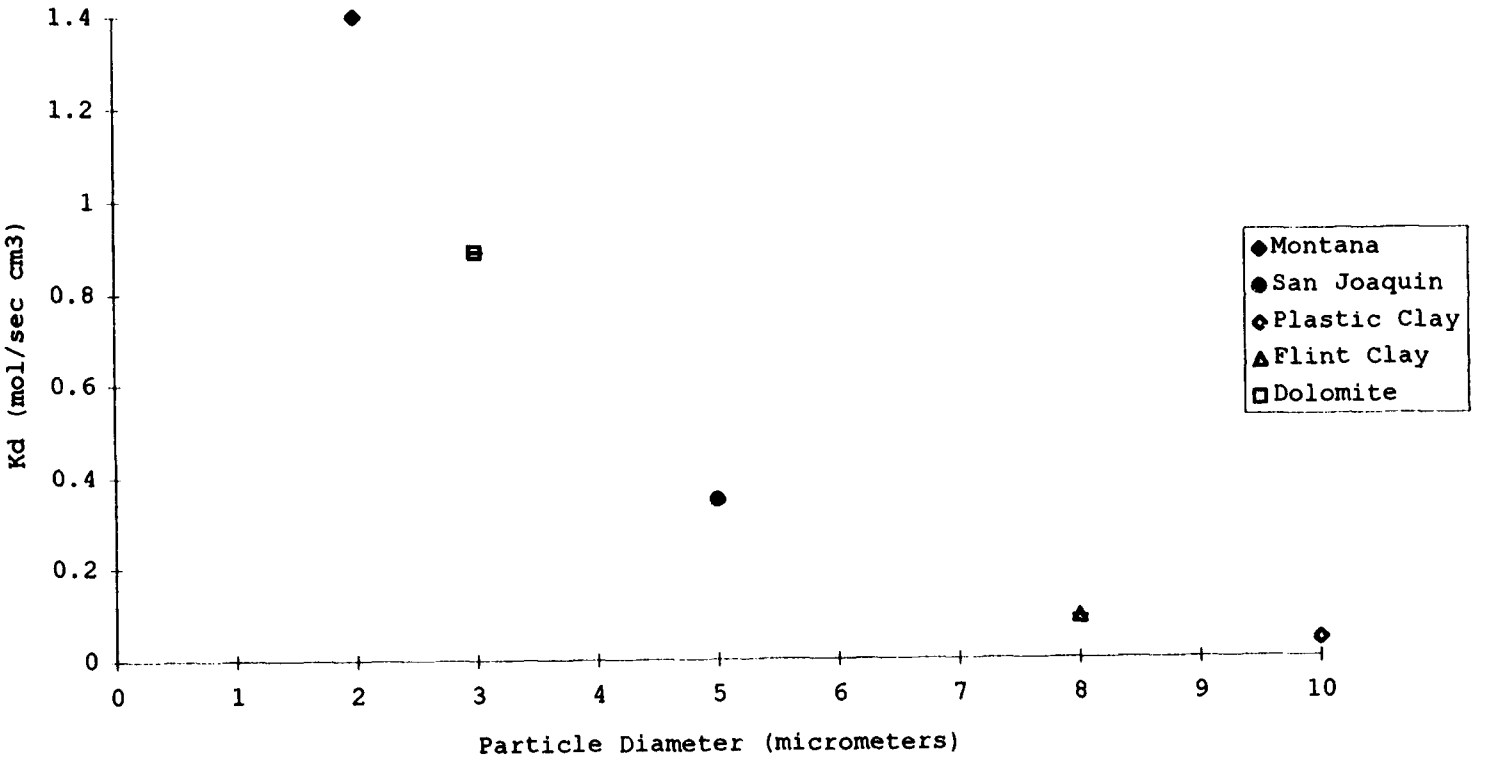

Figure 28. Particle Diameter vs. Kd

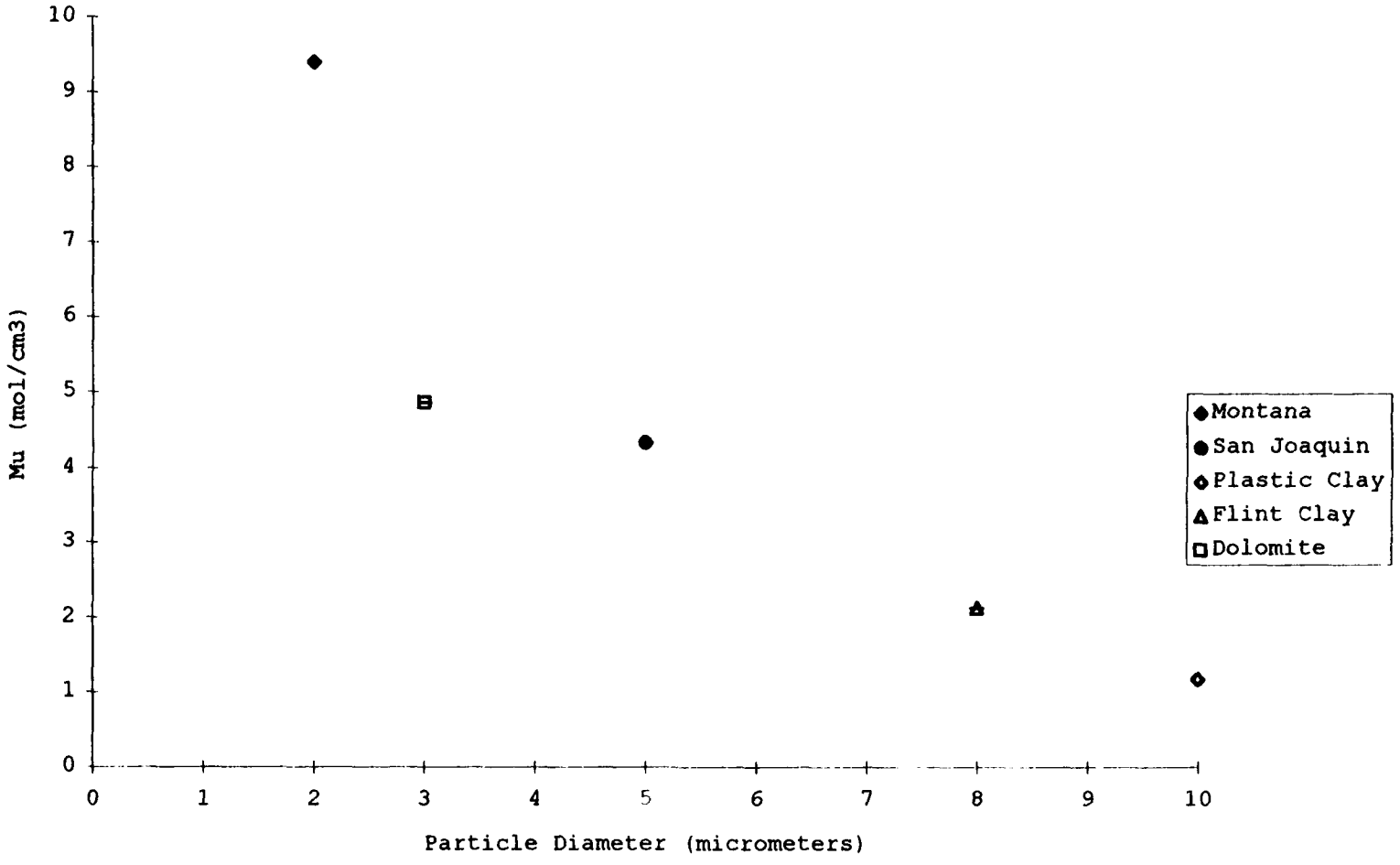

Figure 29. Particle Diameter vs. Mu

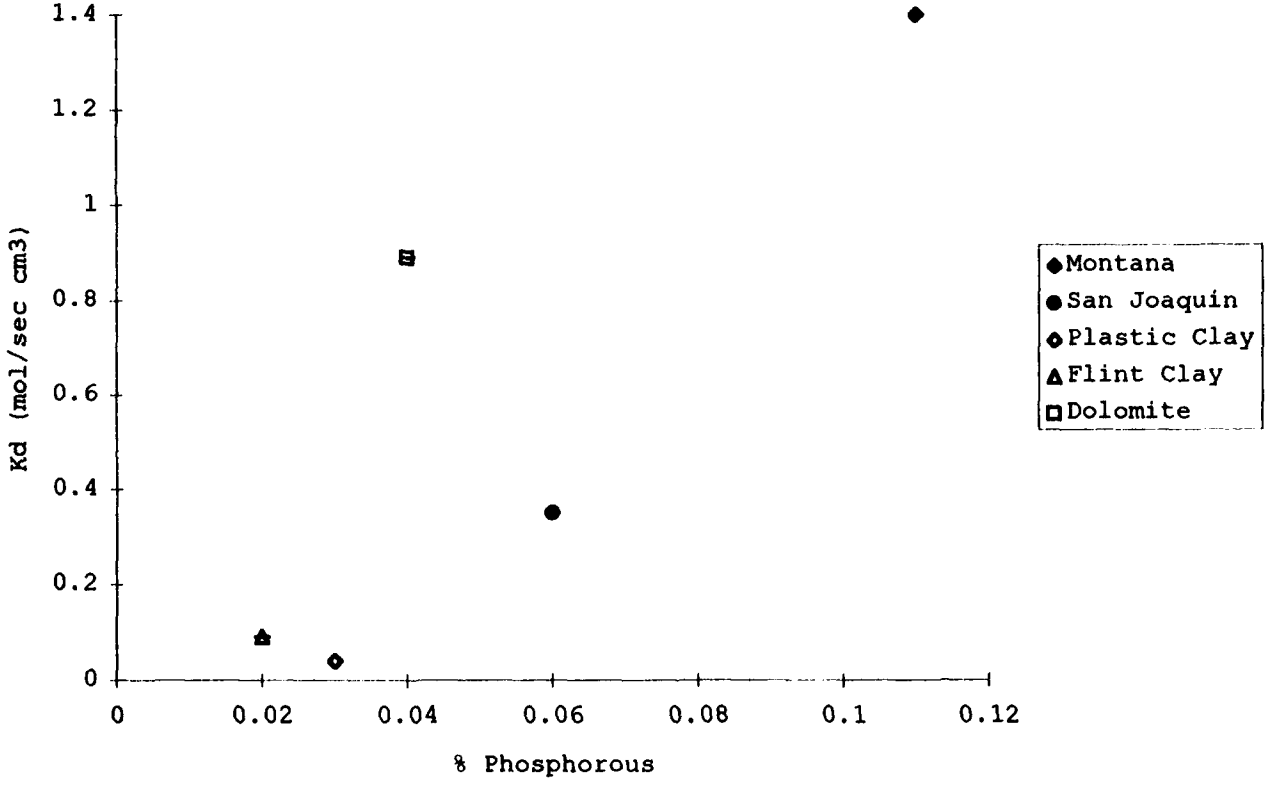

Figure 30. % Phosphorous vs. Kd

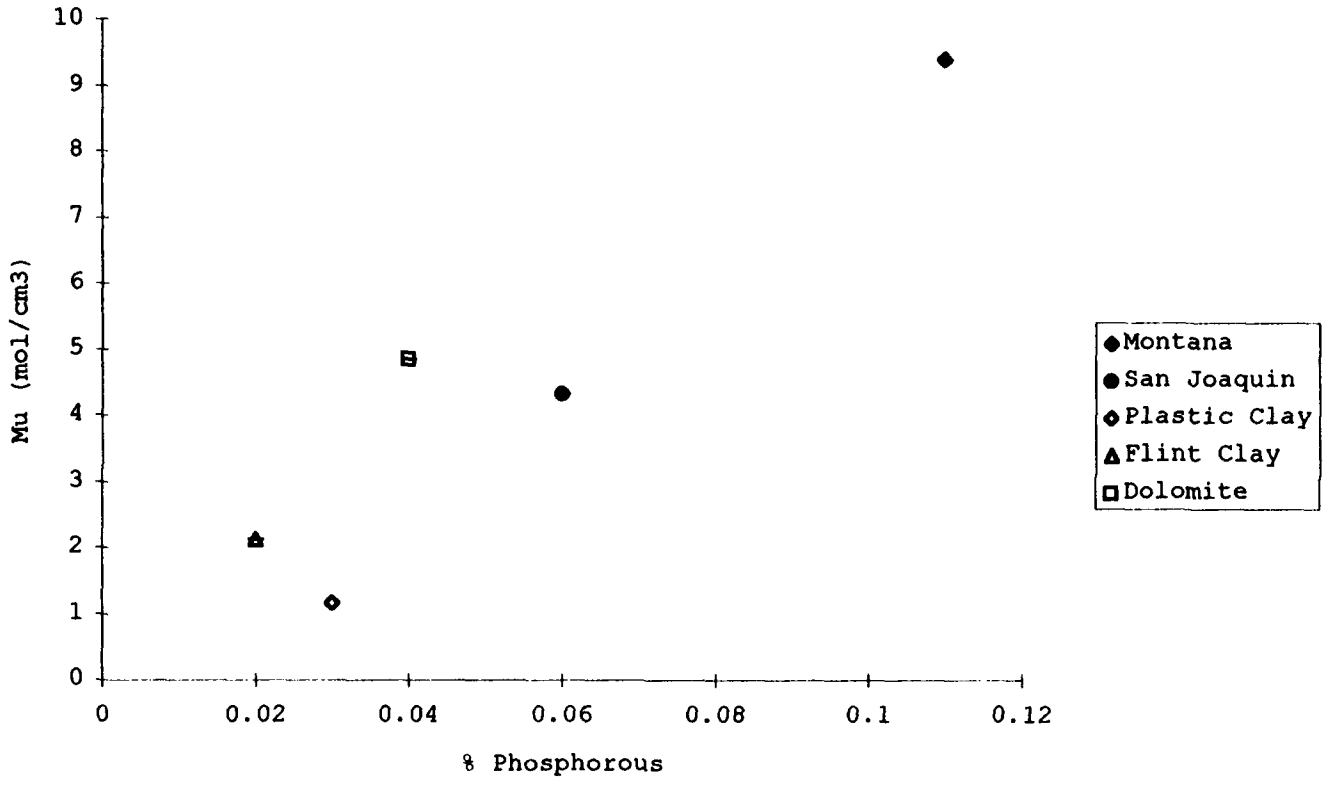

Figure 31. % Phosphorous vs. Mu

V. Conclusions and Recommendations

5.1 Conclusions.

Conclusions were drawn regarding the data gathered by this research. The analysis presented in Chapter 5 of the data gathered from the desorption of TCE from seven types of soil provided insight into each of the research objective established for this thesis.

First, soil characteristics appeared to have a significant impact on both the rate and ultimate progress of TCE desorption. Each of the soils evaluated had very different characteristics and additionally had significantly different K_d and μ values. Moreover, with the majority of the soils evaluated, the differences in characteristics were significantly correlated to corresponding differences in desorption parameters.

The significant negative correlation between particle diameter and both K_d and μ was in keeping with the Langmuir Isotherm theory regarding desorption presented in the literature. The smaller the average particle diameter was of a soil sample, the greater the total surface area was of that sample. From the results of this research, it appears that both the magnitude and rate of desorption were greater with increased total soil surface area. Apparently, the number of sorption sites was directly proportional to the total soil surface area. Thus, by simply looking at the average soil grain sizes of different types of soils, it appears that one would be able to predict differences between their expected desorption rates.

The elemental composition of the soil also appeared to play a significant role in the desorption mechanism. However, it was not clear from the data exactly how the different combinations of elements

interacted to influence desorption. Nonetheless, the presence of certain elements did appear to exert a significant affect on desorption. One possibility is that the ionic charges of the different metallic elements that made up the soil interacted in some way to help or hinder the progress of TCE molecules through the soil matrix. Additionally, this research was able to identify which elements appeared to increase the value of the desorption parameters and which tended to limit desorption. Knowledge of these influences might have predictive value when applied to other soils of different compositions. For instance, soils with high aluminum content would be expected to be slow desorbers, while soils with high sulfur might be expected to desorb TCE more rapidly.

The progress of the desorption from each of the soil samples appeared to be as predicted by the Langmuir Isotherm model. Overall, 5 out of the seven samples fitted to the functional form of the Langmuir Isotherm reported a correlation of over 50%. Additionally, the reason for the curve fit failure with the glass sand may have been due to difficulty in measuring the extremely small quantity (<1 torr) of TCE desorbed by the sample.

Evaluation of the data gathered in the controlled conditions used applied during this research appears to indicated that the Langmuir Isotherm was a valid model for desorption of TCE from soil. The general shape of the concentration versus time plots also appeared to be as predicted. Each of the 5 soils fitting to the Langmuir Isotherm functional form exhibited a rapid initial desorption phase followed by slower desorption decreasing to an asymptotic value. When modeling the fate and transport of TCE contamination in the environment, it appears that the Langmuir Isotherm model would have significant predictive value in tracking the slow desorption process.

Finally, the optical measurement apparatus designed and employed in this research appeared to be an extremely effective tool for use in the study of microscopic physical processes. Using optical measurement techniques allowed the effective isolation and study of TCE activity within the sample cell. Use of light intensity measurements eliminated the need to rely of pressure data that could not be screened for the effects of small pressure leaks or activity of other chemical contaminants within the cell. The apparatus allowed accurate measurement of changes in TCE pressure as small as 1 torr and enabled study of a wide range of soil characteristics over the relatively short time allowed for this research.

Another advantage of the apparatus was its versatility. In addition to study of the influence of soil characteristics upon desorption, the device was readily configurable to study samples at different temperatures or contamination times. The apparatus could also be reconfigured to study the desorption of other VOCs by simply redesigning bandpass filters placed over the InSb detectors.

5.2 Recommendations.

A number of recommendations may be made regarding future application of the results of this thesis. Although every effort was made to incorporate improvements in methodology or experimental design into the present research efforts, the results of this research illuminate additional tasks to performed.

First, additional study of the TCE desorption process is needed. The assumption that the desorption process was concluded within the first 36 hours of observation needs to be validated. It is possible that additional slow desorption would have occurred from the sample over

the next weeks or months. Also, additional insight into the influence of soil chemistry upon desorption is needed. Although a soil chemistry was determined to have a significant affect on desorption, the exact nature of this effect is not yet understood. Finally, soils with different combinations of characteristics could be used to further test the validity of the correlations measured in this research and to determine if there are additional characteristics influencing desorption.

Second, investigation of the utility of using pressure measurement instead of optical techniques might be useful. Although each of the sample cells used in this research exhibited small pressure leaks, redesign of the apparatus might effectively eliminate these leaks, allowing researchers to measure changes in TCE concentration by measuring pressure changes. Although the optical techniques applied in this research were shown to be very effective, the apparatus used was complex and required significant maintenance. By using pressure change measurements alone, the amount of operations and maintenance effort required for data acquisition would be greatly reduced and the data acquisition rate might be increased.

Third, additional research should be done regarding the effects of carbon upon the sorption characteristics of soil. The elemental composition data provided with the soil samples did not include the percent by weight carbon for all of the soils. In some soils (particularly clays), carbon could represent a substantial portion of the total elemental composition and thus might have a significant effect on the sorption of TCE. Other soils with little or no carbon (such as sands) would not experience the influence of carbon and hence might have significantly different sorption characteristics. Other indicators of carbon such as data from loss on ignition (LOI) testing could also be

evaluated.

Finally, the application of the optical techniques used in this research to measurement applications in the field or in environmental laboratories should be investigated. Current measurement technique such as the purge and trap method are unable to measure the sorbed phase contaminants in a soil sample, leading to significant underreporting of contaminant concentrations. Use of optical techniques might improve the accuracy of soil analysis and assist in more effective environmental site assessment and remedial design.

APPENDIX A. Data Acquisition Source Code

```
1  static double volt_one;
2  static double volt_zero;
3  static double volt_two;
4  static double volt_three;
5  static double volt_four;
6  static double volt_five;
7  static double volt_six;
8  static int num_samples;
9   static double volt0[3000], volt1[3000], volt2[3000], volt3[3000],
    volt4[3000];
10  static double volt5[3000],volt6[3000];
11
12  char filename[41];
13
14  static int num_samples;
15  static int wait;
16  static int result;
17  static int close_error;
18  static int byte0;
19  static int byte1;
20  static int byte2;
21  static int byte3;
22  static int byte4;
23  static int byte5;
24  static int byte6;
25   static int handle_zero, handle_one, handle_two, handle_three;
26  static int handle_four, handle_five, handle_six;
27  static int board_code;
28  static int error;
29  static int gain[7];
30  static int chan[7];
31  static int volt_buffer[70];
32
33
34
35
36  main()
37  {
38      int p,m,n;
39      int i,j,z;
40      int x;
41      int q;
42      int point;
43      result = DeleteFile ("volt0.dat");
44      result = DeleteFile ("volt1.dat");
45      result = DeleteFile ("volt2.dat");
46      result = DeleteFile ("volt3.dat");
47      result = DeleteFile ("volt4.dat");
48      result = DeleteFile ("volt5.dat");
49      result = DeleteFile ("volt6.dat");
50
51      error = Init_DA_Brds (1, &board_code);
52      error = MIO_Config (1, 0, 0);
53
54      error = AI_Configure (1, -1, 0, 20, 0, 0);
```

```
55      MIO_Calibrate (1, 1, 0, 6, 0, 0, 0, 8.0, 3);
56
57      cls ();
58
59      n=0;
60      while (n != 1) {
61    FmtOut ("Enter file name (include *.dat extension):  ");
62          n = ScanIn ("%l>%s[w40q]", filename);
63      }
64      DeleteFile (filename);
65
66      cls ();
67
68      p=0;
69      while (p != 1) {
70          FmtOut ("Enter number of samples desired:  ");
71          p = ScanIn ("%l>%i", &num_samples);
72    }
73    cls ();
74
75    m=0;
76    while (m !=1) {
77    FmtOut ("Enter the delay between samples desired (seconds):  ");
78        m = ScanIn ("%l>%i", &wait);
79      }
80    cls ();
81
82    chan[0]=0;
83    chan[1]=1;
84    chan[2]=2;
85    chan[3]=3;
86    chan[4]=4;
87    chan[5]=5;
88    chan[6]=6;
89
90    cls ();
91
92
93    FmtOut ("Pres 1    Temp 1       Lock 1      Pres 2
      Temp 2      Lock 2       Lock 3 \n");
94
95    for (x=0; x<num_samples; x++)
96    {
97    error = AI_VRead (1, 0, -1, &volt_zero);
98    error = AI_VRead (1, 1, 100, &volt_one);
99    error = AI_VRead (1, 2, 100, &volt_two);
100   error = AI_VRead (1, 3, -1, &volt_three);
101   error = AI_VRead (1, 4, -1, &volt_four);
102   error = AI_VRead (1, 5, -1, &volt_five);
103   error = AI_VRead (1, 6, -1, &volt_six);
104
105   volt0[x]=volt_zero*10+.05;
106
107
108   volt1[x]= 28 + 0.226584602 + volt_one * (24152.109 + volt_one *
109   (67233.4248 + volt_one * (2210340.682 + volt_one *
110   (-860963914.9 + volt_one * (4.83506E+10 + volt_one *
111   (-1.18452E+12 + volt_one * (1.38690E+13 + volt_one *
112   -6.33708E+13)))))));
```

```
113
114   volt2[x]= 28 + 0.226584602 + volt_two * (24152.109 + volt_two *
115   (67233.4248 + volt_two * (2210340.682 + volt_two *
116   (-860963914.9 + volt_two * (4.83506E+10 + volt_two *
117   (-1.18452E+12 + volt_two * (1.38690E+13 + volt_two *
118   -6.33708E+13)))))));
119
120   volt3[x]=volt_three*.5;
121   volt4[x]=volt_four*.5;
122   volt5[x]=volt_five*10;
123   volt6[x]=volt_six*10-0.1;
124
125
126   FmtOut ("%f[p2]       %f[p2]      %f[p4]       %f[p2]
      %f[p2]", volt0[x], volt1[x], volt3[x], volt6[x], volt2[x]);
127   FmtOut ("      %f[p4]      %f[p4] \n", volt4[x], volt5[x]);
128
129   handle_zero = OpenFile (filename, 2, 1, 1);
130   SetFilePtr (handle_zero, 0L, 0);
131   FmtFile (handle_zero,"%f, %f, %f, %f, %f, %f, %f\n",volt0[x],
      volt1[x], volt3[x], volt6[x], volt2[x], volt4[x], volt5[x]);
132   CloseFile (handle_zero);
133
134   delay (wait);
135
136   }
137   }
```

APPENDIX B. Soil Characteristics Data

National Bureau of Standards

Certificate of Analysis

Standard Reference Material 88b

Dolomitic Limestone

This Standard Reference Material (SRM) is intended for use in the analysis of rocks, ores, minerals, and materials of similar matrix. SRM 88b is a powdered limestone that was passed through a No. 60 sieve (nominal sieve opening of 250 μm). Limestone is a major industrial raw material for the cement and refractory materials industries (including the steel industry). The control of constituents in limestone is essential to the quality control of the product and product additives.

The certified constituents for SRM 88b are given in Table 1. The certified values are based on measurements using two or more independent reliable methods or techniques. Noncertified values for constituent elements are given in Table 2 as additional information on the composition. The noncertified values should not be used for calibration or quality control. For user convenience gravimetric factors for converting the oxides to elements are given in Table 3. All values are based on samples that were dried for 2 hours at 110 °C and a minimum sample size of 250 mg.

Table 1
Certified Values for Constituents

Constituent[1]	Content, Wt. %[2]	Constituent	Content, Wt. %
Al_2O_3[c,g,h,k]	0.336 ± 0.013	MgO[c,g,h]	21.03 ± 0.07
CaO[c,g]	29.95 ± 0.05	Na_2O[a,e,f,k]	0.0290 ± 0.0007
CO_2[d,g,i]	46.37 ± 0.12*	P_2O_5[b,h]	0.0044 ± 0.0003*
Fe_2O_3[a,b,e,h,j] (Total Fe as Fe_2O_3)	0.277 ± 0.002	SiO_2[e,g,h]	1.13 ± 0.02
K_2O[a,e,f,j]	0.1030 ± 0.0024	SrO[a,e,f,j]	0.0076 ± 0.0003
MnO[a,b,h]	0.0160 ± 0.0012		

[1] Methods/Techniques
[a] Atomic Absorption Spectrometry
[b] Colorimetry
[c] Complexometric Titration
[d] Coulometry
[e] DC Plasma Emission Spectrometry
[f] Flame Emission Spectrometry
[g] Gravimetry
[h] Inductively Coupled Plasma Atomic Emission Spectrometry
[i] Inert Gas Fusion
[j] Isotope Dilution Mass Spectrometry
[k] Neutron Activation Analysis

[2] The listed uncertainty, unless otherwise noted, is ± two standard deviations of the certified value. The uncertainty primarily reflects differences between the various methods of analyses.
* The statistically derived uncertainty was extremely small for this constituent. The uncertainty is based on judgment and approximates ± two standard deviations.

October 9, 1987
Gaithersburg, MD 20899
(Revision of Certificate
dated April 21, 1986)

Stanley D. Rasberry, Chief
Office of Standard Reference Materials

(over)

Table 2
Noncertified Values for Constituents

Constituent	Content, μg/g	Constituent	Content, wt. %
CeO_2[k]	(4.7)	TiO_2[e,f]	(0.016)
CoO[k]	(1.3)		
Cr_2O_3[k]	(3.4)		
Cs_2O[k]	(0.17)	LOI[g] (1000 °C for 18 hrs)	(46.98)
Eu_2O_3[k]	(0.15)		
HfO_2[k]	(0.16)	H_2O[g] (110 °C for 2 hrs)	(0.24)
Sc_2O_3[k]	(0.56)		
ThO_2[k]	(0.35)		

Table 3
Gravimetric Factors Used for Conversion of Oxides to Elements
(Compiled from International Atomic Weights of 1985)

Constituent	Gravimetric Factor	Constituent	Gravimetric Factor
Al_2O_3	0.52925	K_2O	0.83015
CaO	.71469	MnO	.77446
CeO_2	.81408	MgO	.60304
CO_2	.27292	Na_2O	.74186
CoO	.78648	P_2O_5	.43642
Cr_2O_3	.68420	Sc_2O_3	.65196
Cs_2O	.94323	SiO_2	.46743
Eu_2O_3	.86361	SrO	.84559
Fe_2O_3	.69943	ThO_2	.87881
HfO_2	.84798	TiO_2	.59941

PLANNING, PREPARATION, TESTING, AND ANALYSIS:
The material for this SRM was provided by Material Service Corporation, Chicago, Illinois. The source of the material was a mine near Skokie, Illinois. The material was received at NBS as a fine powder, 80 to 100 percent passing a 200 mesh sieve. At NBS the material was sieved with a No. 60 sieve, blended, and placed in polyethylene lined aluminum cans for bulk storage.

Samples from the top and bottom of each can were analyzed, using x-ray fluorescence, to establish homogeneity of the material. Seven elements, Mg, Fe, Ti, Cu, Si, K, and Al were determined in 18 randomly selected samples of SRM 88b and no significant differences between samples were found for any of the measured elements.

Homogeneity testing was performed by G.A. Sleater of the Gas and Particulate Science Division.

Chemical analyses for certification were performed in the following laboratories:

National Bureau of Standards, Center for Analytical Chemistry, Gaithersburg, MD, D.A. Becker, T.A. Butler, Mo De-Ming, B.I. Diamondstone, R.C. Gauer, J.W. Gramlich, Yie Guirong, J.D. Fassett, J.R. Moody, P.A. Pella, T.C. Rains, T.A. Rush, G.A. Sleater, R.L. Watters, Jr., and Y.Z. Zhang.

Mineral Constitution Laboratory, Pennsylvania State University, University Park, Pennsylvania, J.B. Bodkin, J.C. Devine and H. Gong.

The statistical analysis of the data for certification was performed by R.C. Paule, National Measurement Laboratory.

The technical and support aspects involved in the preparation, certification, and issuance of this Standard Reference Material were coordinated through the Office of Standard Reference Materials by T.E. Gills.

U.S. Department of Commerce
C. William Verity
Secretary

National Bureau of Standards

Certificate of Analysis

Standard Reference Material 97b

Flint Clay

This Standard Reference Material (SRM) is intended for use in the determination of constituent elements in clay or material of similiar matrix. SRM 97b is powdered clay that was air-dried, ball-milled, and blended to ensure homogeneity.

The certified constituent elements of SRM 97b are given below in Table 1. The certified values are based on measurements made using two or more independent reliable methods or techniques. Non-certified values for constituent elements are given in Table 2 as additional information on the composition. The non-certified values should not be used for calibration or quality control. All values are based on samples that were dried for 2 hours in a conventional oven at 140 °C and a minimum sample size of 250 mg.

Table 1

Certified Values for Constituent Elements

Element[1]	Content, Wt. %[2]	Element	Content, Wt. %
Aluminum [c,d,g]	20.76 ± 0.15	Manganese [b,g]	0.0047 ± 0.0005
Calcium [b,d,f]	0.0249 ± 0.0026	Potassium [b,c,f,g,i]	0.513 ± 0.023
Chromium [c,g]	0.0227 ± 0.0012	Silicon [e,i]	19.81 ± 0.04
Iron [c,g]	0.831 ± 0.008	Sodium [b,d,g]	0.0492 ± 0.0023
Lithium [d,f]	0.055 ± 0.001	Strontium [d,f,g]	0.0084 ± 0.0002
Magnesium [b,c]	0.113 ± 0.002	Titanium [b,g,h,i]	1.43 ± 0.04

[1] Methods / Techniques

a Colorimetry (o-phenanthroline)
b DC Plasma Spectrometry
c Flame Atomic Absorption Spectrometry
d Flame Emission Spectrometry
e Gravimetry
f Isotope Dilution Mass Spectrometry
g Instrumental Neutron Activation Analysis
h Spectrophotometry
i X-ray Fluorescence

[2] The certified value is a weighted mean of results from two or more analytical techniques. The weights for the weighted means were computed according to the iterative procedure of Paule and Mandel (NBS Journal of Research 87, 1982, pp. 377-385). The uncertainty is the sum, in quadrature, of the half-width of a 95% expected tolerance interval and an allowance for systematic error among the methods used. The interval whose endpoints are the certified value minus and plus the uncertainty, respectively, will cover the concentration in a minimum sample size of 250 mg of this SRM for at least 95% of the samples with 95% confidence.

Gaithersburg, MD 20899
April 21, 1988

Stanley D. Rasberry, Chief
Office of Standard Reference Materials

(over)

Table 2

Non-certified Values for Constituent Elements

Element	Content, Wt.%	Element	Content, Wt%
Barium	(0.018)	Zirconium	(0.05)
Phosphorus	(0.02)		

Element	Content, µg/g	Element	Content, µg/g
Antimony	(2.2)	Rubidium	(33)
Cesium	(3.4)	Scandium	(22)
Cobalt	(3.8)	Thorium	(36)
Europium	(0.84)	Zinc	(87)
Hafnium	(13)		
		Loss on Ignition	(13.3 wt%)

Loss on ignition was obtained by igniting sample for 2 hours at 1100 °C after sample was dried for two hours at 140 °C.

Source and Preparation

The flint clay for SRM 97b was donated to NBS by F.J. Flanagan and J.W. Hassman of the United States Geological Survey, Reston, Virginia. Approximately 220 kg of flint clay was collected from a stockpile near the Harbison-Walker Refractories Co. Mine on Anderson Creek, Pike Township, Clearfield County, PA. The collected clay was air-dried and processed by the same method used to prepare USGS rock standards (USGS Bulletin 1582, Flanagan, 1986). After processing, the sample was delivered to NBS, where it was again mixed in a 0.3 cubic meter "V" blender for approximately 45 minutes. After blending the clay was placed in polyethylene lined aluminum pails and subsequently bottled.

Homogeneity testing was performed using x-ray fluorescence and instrumental activation analysis on randomly selected samples from cans of bulk material. There were no significant differences among samples for any of the measured elements.

Chemical analyses were performed in the following laboratories:

- National Bureau of Standards, Center for Analytical Chemistry, E.S. Beary, D.A. Becker, W.A. Bowman III, T.A. Butler, K.A. Brletic, J.W.Gramlich, D. Mo, J.R. Moody, and T.C. Rains.

- Mineral Constitution Laboratory, Pennsylvania State University, University Park, Pennsylvania, J.B. Bodkin.

- Engelhard Corporation, Specialty Chemical Division, Edison, New Jersey, B.P. Scibek.

- Construction Technology Laboratories, Inc., Skokie, Illinois, H.M. Kanare.

The statistical analysis and evaluation of the data for certification was performed by K.R. Eberhardt and S.B. Schiller of the Statistical Engineering Division and R.L. Watters, Jr. of the Inorganic Analytical Research Division.

The technical and support aspects involved in the preparation, certification, and issuance of this Standard Reference Material were coordinated through the Office of Standard Reference Materials by T.E. Gills.

U.S. Department of Commerce
Juanita M. Kreps
Secretary

National Bureau of Standards
Ernest Ambler, Acting Director

National Bureau of Standards Certificate of Analysis

Standard Reference Material 81a

Glass Sand

(In Cooperation with the American Society for Testing and Materials)

This SRM is issued in the form of a ground powder (95% less than 106 μm) blended to ensure homogeneity. It should be dried for 2 hours at 105 °C before use.

Constituent	Recommended Value Percent by Weight	Range	s
Al_2O_3	0.66	0.62 - 0.69	0.011
Fe_2O_3	.082	.075 - .089	.0024
TiO_2	.12	.10 - .14	.0064
ZrO_2	.034	.025 - .042	.0026
Cr_2O_3	46 μg/g	33 - 58	3.9

Certification - The recommended value listed for each oxide is the best estimate of the true value based on the analytical data from both cooperators and NBS. The range of values listed is the tolerance interval, constructed such that it will cover at least 95% of the population with a probability of 0.99. It is computed as $X \pm Ks$: where s is the standard deviation, K is a factor that depends on n (the number of samples measured), p, the proportion of the total sample covered (95%), and γ, the probability level (99%). In all cases none of the n values used exceeded the range specified. Thus, it includes variability between laboratories and between samples.

The overall direction and coordination of the round-robin analysis leading to certification were performed by Paul Close, Chairman of ASTM Subcommittee C-14.02 on Chemical Analysis of Glass and Glass Products.

The technical and support aspects involved in the preparation, certification, and issuance of this Standard Reference Material were coordinated through the Office of Standard Reference Materials by W. P. Reed.

Washington, D.C. 20234
January, 1978

J. Paul Cali, Chief
Office of Standard Reference Materials

(over)

Chemical analyses for certification were performed in the following laboratories:

Anchor Hocking Corp., Lancaster, Ohio, R. E. Carr
Brockway Glass Co., Inc., Brockway, Pa., E. L. McKinley.
Corning Glass Works, Corning, N.Y., Y. S. Su.
Ford Motor Co., Lincoln Park, Mich., T. O. LaFramboise.
National Bureau of Standards, Analytical Chemistry Division, E. J. Maienthal, J. D. Messman and T. C. Rains.
Kimble Div. Owens-Illinois, Vineland, N. J., H. S. Moser.
Owens-Illinois, Inc., Toledo, Ohio, P. Close.
Penn State Univ., University Park, Pa., J. B. Bodkin.

National Institute of Standards & Technology

Certificate of Analysis

Standard Reference Material 2710

Montana Soil

Highly Elevated Trace Element Concentrations

This Standard Reference Material (SRM) is intended primarily for use in the analysis of soils, sediments, or other materials of a similar matrix. SRM 2710 is a highly contaminated soil that was oven-dried, sieved, and blended to achieve a high degree of homogeneity. A unit of SRM 2710 consists of 50 g of the dried material.

The certified elements for SRM 2710 are given in Table 1. The values are based on measurements using one definitive method or two or more independent and reliable analytical methods. Noncertified values for a number of elements are given in Table 2 as additional information on the composition. The noncertified values should not be used for calibration or quality control. Analytical methods used for the characterization of this SRM are given in Table 3 along with analysts and cooperating laboratories. All values (except for carbon) are based on measurements using a sample weight of at least 250 mg. Carbon measurements are based on 100-mg samples.

NOTICE AND WARNINGS TO USERS

Expiration of Certification: This certification is valid for 5 years from the date of shipment from NIST. Should any of the certified values change before the expiration of the certification, purchasers will be notified by NIST. Return of the attached registration card will facilitate notification.

Stability: This material is considered to be stable; however, its stability has not been rigorously assessed. NIST will monitor this material and will report any substantive changes in certification to the purchaser.

Use: A minimum sample weight of 250 mg (dry weight - see Instructions for Drying) should be used for analytical determinations to be related to the certified values on this Certificate of Analysis.

To obtain the certified values, sample preparation procedures should be designed to effect complete dissolution. If volatile elements (i.e., Hg, As, Se) are to be determined, precautions should be taken in the dissolution of SRM 2710 to avoid volatilization losses.

Statistical consultation was provided by S.B. Schiller of the NIST Statistical Engineering Division.

The overall direction and coordination of the analyses were under the chairmanship of M.S. Epstein and R.L. Watters, Jr., of the NIST Inorganic Analytical Research Division.

The technical and support aspects involved in the preparation, certification, and issuance of this Standard Reference Material were coordinated through the Standard Reference Materials Program by T.E. Gills and J.S. Kane.

Gaithersburg, MD 20899
October 30, 1992

William P. Reed, Chief
Standard Reference Materials Program

(over)

Instructions for Drying: When nonvolatile elements are to be determined, samples should be dried for 2 h at 110 °C. Volatile elements (i.e., Hg, As, Se) should be determined on samples as received; separate samples should be dried as previously described to obtain a correction factor for moisture. Correction for moisture is to be made to the data for volatile elements before comparing to the certified values. This procedure ensures that these elements are not lost during drying. The weight loss on drying has been found to be in the range of 1.7 to 2.3 %.

Source and Preparation of Material: The U.S. Geological Survey (USGS), under contract to the NIST, collected and processed the material for SRM 2710. The soil was collected from the top 10 cm (4 in) of pasture land located at Longitude 112° 47' and Latitude 46° 01' along Silver Bow Creek in the Butte, Montana area. The site is approximately nine miles east of the local Anaconda plant and 6.5 miles south of settling ponds that feed the creek. The creek periodically floods, depositing sediment with high concentrations of copper, manganese, and zinc at the collection site. The material was shoveled from a 6.1 m x 6.1 m (20 ft x 20 ft) area into polyethylene bags in cardboard cartons for shipment to the USGS laboratory for processing.

The material was spread on 30.5 cm x 61 cm (1 ft x 2 ft) polyethylene-lined drying trays in an air drying oven and dried for three days at room temperature. The material was then passed over a vibrating 2-mm screen to remove plant material, rocks, and large chunks of aggregated soil. Material remaining on the screen was deaggregated and rescreened. The combined material passing the screen was ground in a ball mill to pass a 74-μm screen and blended for 24 h. Twenty grab samples were taken and measured for the major oxides using x-ray fluorescence spectrometry and for several trace elements using inductively coupled plasma atomic emission analysis to provide preliminary assessment of the homogeneity of the material prior to bottling. The material was bottled into 50-g units and randomly selected bottles were taken for the final homogeneity testing.

Analysis: The homogeneity, using selected elements in the bottled material as indicators, was assessed using x-ray fluorescence spectrometry and neutron activation analysis. In a few cases, statistically significant differences were observed, and the variance due to material inhomogeneity is included in the overall uncertainties of the certified values. The estimated relative standard deviation for material inhomogeneity is less than 2 % for those elements for which homogeneity was assessed.

Certified Values and Uncertainties: The certified values are weighted means of results from two or more independent analytical methods, or the mean of results from a single definitive method, except for mercury. Mercury certification is based on cold vapor atomic absorption spectrometry used by two different laboratories employing different methods of sample preparation prior to measurement. The weights for the weighted means were computed according to the iterative procedure of Paule and Mandel (NBS Journal of Research 87, 1982, pp. 377-385). The stated uncertainty includes allowances for measurement imprecision, material variability, and differences among analytical methods. Each uncertainty is the sum of the half-width of a 95 % prediction interval and includes an allowance for systematic error among the methods used. In the absence of systematic error, a 95 % prediction interval predicts where the true concentrations of 95 % of the samples of this SRM lie.

Table 1. Certified Values

Element	wt. %			Element	µg/g		
Aluminum	6.44	±	0.08	Antimony	38.4	±	3.0
Calcium	1.25	±	0.03	Arsenic	626	±	38
Iron	3.38	±	0.10	Barium	707	±	51
Magnesium	0.853	±	0.042	Cadmium	21.8	±	0.2
Manganese	1.01	±	0.04	Copper	2950	±	130
Phosphorus	0.106	±	0.015	Lead	5532	±	80
Potassium	2.11	±	0.11	Mercury	32.6	±	1.8
Silicon	28.97	±	0.18	Nickel	14.3	±	1.0
Sodium	1.14	±	0.06	Silver	35.3	±	1.5
Sulfur	0.240	±	0.006	Vanadium	76.6	±	2.3
Titanium	0.283	±	0.010	Zinc	6952	±	91

Noncertified Values: Noncertified values, shown in parentheses, are provided for information only. An element concentration value may not be certified if a bias is suspected in one or more of the methods used for certification, or if two independent methods are not available. Certified values for some of these elements will eventually be provided in a revised certificate when more data is available.

Table 2. Noncertified Values

Element	wt.%	Element	µg/g
Carbon	(3)	Bromine	(6)
		Cerium	(57)
		Cesium	(107)
		Chromium	(39)
		Cobalt	(10)
		Dysprosium	(5.4)
		Europium	(1)
		Gallium	(34)
		Gold	(0.6)
		Hafnium	(3.2)
		Holmium	(0.6)
		Indium	(5.1)
		Lanthanum	(34)
		Molybdenum	(19)
		Neodymium	(23)
		Rubidium	(120)
		Samarium	(7.8)
		Scandium	(8.7)
		Strontium	(240)
		Thallium	(1.3)
		Thorium	(13)
		Tungsten	(93)
		Uranium	(25)
		Ytterbium	(1.3)
		Yttrium	(23)

Table 3. Analytical Methods Used for the Analysis of SRM 2710

Element	Certification Methods *	Element	Certification Methods *
Ag	ID ICPMS; RNAA; INAA	Mo	ID ICPMS
Al	XRF1; XRF2; DCP; ICP	Na	INAA; FAES
As	RNAA; HYD AAS; ICP; INAA	Nd	ICP
Au	INAA; FAAS	Ni	ID ICPMS; ETAAS; INAA
Ba	XRF2; FAES	P	DCP; COLOR; XRF1; XRF2
Br	INAA	Pb	ID TIMS; POLAR; ICP
C	COUL	Rb	INAA
Ca	XRF1; XRF2; DCP	S	ID TIMS
Cd	ID ICPMS; RNAA	Sb	RNAA; ETAAS
Ce	INAA; ICP	Sc	INAA; ICP
Co	INAA; ETAAS; ICP	Si	XRF1; XRF2; GRAV
Cr	INAA; DCP; ICP	Sm	INAA
Cs	INAA	Sr	ID TIMS; INAA; ICP
Cu	RNAA; FAES; ICP	Th	ID TIMS; INAA; ICP
Dy	INAA	Ti	XRF1; XRF2; DCP
Eu	INAA	Tl	ID TIMS; LEAFS
Fe	XRF1; XRF2; DCP; INAA; ICP	U	ID TIMS; INAA
Ga	INAA; ICP	V	INAA; ICP
Hf	INAA	W	INAA
Hg	CVAAS	Y	ICP
Ho	INAA	Yb	INAA
In	INAA	Zn	ID TIMS; ICP; INAA; POLAR
K	XRF1; XRF2; FAES; ICP		
La	INAA; ICP		
Mg	XRF1; ICP		
Mn	INAA; DCP; XRF2		

*Methods in bold were used to corroborate certification methods or to provide information values.

ID TIMS - Isotope dilution thermal ionization mass spectrometry; mixed acid digestion.
ID ICPMS - Isotope dilution inductively coupled plasma mass spectrometry; mixed acid digestion.
INAA - Instrumental neutron activation analysis.
RNAA - Radiochemical neutron activation analysis; mixed acid digestion.
XRF1 - Wavelength dispersive x-ray fluorescence on fused borate discs.
XRF2 - Wavelength dispersive x-ray fluorescence spectrometry on pressed powder.
ICP - Inductively coupled plasma atomic emission spectrometry; mixed acid digestion.
DCP - Direct current plasma atomic emission spectrometry; lithium metaborate fusion.
ETAAS - Electrothermal atomic absorption spectrometry; mixed acid digestion.
CVAAS - Cold vapor atomic absorption spectrometry.
HYD AAS - Hydride generation atomic absorption spectrometry.
FAAS - Flame atomic absorption spectrometry; mixed acid digestion except for Au, leached with HBr-Br_2.
FAES - Flame atomic emission spectrometry; mixed acid digestion.
COLOR - Colorimetry; lithium metaborate fusion.
GRAV - Gravimetry; sodium carbonate fusion.
COUL - Combustion coulometry.
LEAFS - Laser enhanced atomic fluorescence spectrometry; mixed acid digestion.
POLAR - Polarography.

Participating NIST Analysts

M. Adriaens	A. Marlow
E.S. Beary	J.R. Moody
C.A. Beck	P.J. Paulsen
D.S. Braverman	P. Pella
M.S. Epstein	T.A. Rush
J.D. Fassett	J.M. Smeller
K.M. Garrity	G.C. Turk
R.R. Greenberg	T.W. Vetter
W.R. Kelly	R.D. Vocke
R.M. Lindstrom	L.J. Wood
E.A. Mackey	R.L. Watters, Jr.

Participating Laboratories

P. Briggs, D. Siems, J. Taggart, S. Wilson
U.S. Geological Survey
Branch of Geochemistry
Denver, CO 80225

J.B. Bodkin
College of Earth and Mineral Sciences
The Pennsylvania State University
University Park, PA 16802

S.E. Landsberger, V.G. Vermette
Department of Nuclear Engineering
University of Illinois
Urbana, IL 61801

...ment of Commerce
William Verity
Secretary

...Bureau of Standards
...Director

National Bureau of Standards

Certificate of Analysis

Standard Reference Material 98b

Plastic Clay

This Standard Reference Material (SRM) is intended for use in the determination of constituent elements in clay or material of similar matrix. SRM 98b is powdered clay that was air-dried, ball-milled, and blended to ensure homogeneity.

The certified constituent elements of SRM 98b are given below in Table 1. The certified values are based on measurements made using two or more independent reliable methods or techniques. Non-certified values for constituent elements are given in Table 2 as additional information on the composition. The non-certified values should not be used for calibration or quality control. All values are based on samples that were dried for 2 hours in a conventional oven at 140 °C and a minimum sample size of 250 mg.

Table 1

Certified Values for Constituent Elements

Element[1]	Content, Wt. %[2]	Element	Content, Wt.%
Aluminum [c,d,g]	14.30 ± 0.20	Manganese [b,g]	0.0116 ± 0.0005
Calcium [b,d,f]	0.0759 ± 0.0035	Potassium [b,c,f,g,i]	2.81 ± 0.07
Chromium [c,g]	0.0119 ± 0.0005	Silicon [e,i]	26.65 ± 0.16
Iron [c,g]	1.18 ± 0.01	Sodium [b,d,g]	0.1496 ± 0.0066
Lithium [d,f]	0.0215 ± 0.0003	Strontium [d,f,g]	0.0189 ± 0.0008
Magnesium [b,c]	0.358 ± 0.012	Titanium [b,g,i]	0.809 ± 0.012

[1] Methods/Techniques

a Colorimetry (o-phenanthroline)
b DC Plasma Spectrometry
c Flame Atomic Absorption Spectrometry
d Flame Emission Spectrometry
e Gravimetry
f Isotope Dilution Mass Spectrometry
g Instrumental Neutron Activation Analysis
h Spectrophotometry
i X-ray Fluorescence

[2] The certified value is a weighted mean of results from two or more analytical techniques. The weights for the weighted means were computed according to the iterative procedure of Paule and Mandel (NBS Journal of Research 87, 1982, pp. 377-385). The uncertainty is the sum, in quadrature, of the half-width of a 95% expected tolerance interval and an allowance for systematic error among the methods used. The interval whose endpoints are the certified value minus and plus the uncertainty, respectively, will cover the concentration in a minimum sample size of 250 mg of this SRM for at least 95% of the samples with 95% confidence.

Gaithersburg, MD 20899
April 21, 1988

Stanley D. Rasberry, Chief
Office of Standard Reference Materials

(over)

Table 2

Non-certified Values for Constituent Elements

Element	Content, Wt%	Element	Content, Wt%
Barium	(0.07)	Rubidium	(0.018)
Phosphorus	(0.03)	Zinc	(0.011)
		Zirconium	(0.022)

Element	Content, μg/g	Element	Content, μg/g
Antimony	(1.6)	Hafnium	(7.2)
Cesium	(16.5)	Scandium	(22)
Cobalt	(16.3)	Thorium	(21)
Europium	(1.3)		

Loss on Ignition (7.5 wt.%)

Loss on ignition was obtained by igniting sample for two hours at 1100 °C after sample was dried for two hours at 140 °C.

Source and Preparation

The plastic clay for SRM 98b was donated to NBS by F.J. Flanagan and J.W. Hasterman of the United States Geological Survey, Reston, Virginia. Approximately 220 kg of plastic clay was collected from the underclay of the Clarion coal bed at the Harbison-Walker Refractories Co. plant at Clearfield, Clearfield County, PA. The collected clay was air-dried and processed by the same method used to prepare USGS rock standards (USGS Bulletin 1582, Flanagan 1986). After processing, the sample was delivered to NBS, where it was again mixed in a 0.3 cubic meter "V" blender for approximately 45 minutes. After blending the clay was placed in polyethylene lined aluminum pails and subsequently bottled.

Homogeneity testing was performed using x-ray fluorescence and instrumental activation analysis on samples randomly selected samples from cans of bulk material. There were no significant differences between samples for any of the measured elements.

Chemical analyses were performed in the following laboratories:

- National Bureau of Standards, Center for Analytical Chemistry, E.S. Beary, D.A. Becker, W.A. Bowman III, T.A. Butler, K.A. Brletic, J.W. Gramlich, D. Mo, J.R. Moody, and T.C. Rains.

- Mineral Constitution Laboratory, Pennsylvania State University, University Park, Pennsylvania, J.B. Bodkin.

- Engelhard Corporation, Specialty Chemical Division, Edison, New Jersey, B.P. Scibek.

- Construction Technology Laboratories, Inc., Skokie, Illinois, H.M.Kanare.

The statistical analysis and evaluation of the data for certification was performed by K.R. Eberhardt and S.B. Schiller of the Statistical Engineering Division and R.L.Watters, Jr. of the Inorganic Analytical Research Division.

The technical and support aspects involved in the preparation, certification, and issuance of this Standard Reference Material were coordinated through the Office of Standard Reference Materials by T.E. Gills.

National Institute of Standards & Technology

Certificate of Analysis

Standard Reference Material 2709

San Joaquin Soil

Baseline Trace Element Concentrations

This Standard Reference Material (SRM) is intended primarily for use in the analysis of soils, sediments, or other materials of a similar matrix. SRM 2709 is an agricultural soil that was oven-dried, sieved, and blended to achieve a high degree of homogeneity. A unit of SRM 2709 consists of 50 g of the dried material.

The certified elements for SRM 2709 are given in Table 1. The values are based on measurements using one definitive method or two or more independent and reliable analytical methods. Noncertified values for a number of elements are given in Table 2 as additional information on the composition. The noncertified values should not be used for calibration or quality control. Analytical methods used for the characterization of this SRM are given in Table 3 along with analysts and cooperating laboratories. All values (except for carbon) are based on measurements using a sample weight of at least 250 mg. Carbon measurements are based on 100-mg samples.

NOTICE AND WARNINGS TO USERS

Expiration of Certification: This certification is valid for 5 years from the date of shipment from NIST. Should any of the certified values change before the expiration of the certification, purchasers will be notified by NIST. Return of the attached registration card will facilitate notification.

Stability: This material is considered to be stable; however, its stability has not been rigorously assessed. NIST will monitor this material and will report any substantive changes in certification to the purchaser.

Use: A minimum sample weight of 250 mg (dry weight - see Instructions for Drying) should be used for analytical determinations to be related to the certified values on this Certificate of Analysis .

To obtain the certified values, sample preparation procedures should be designed to effect complete dissolution. If volatile elements (i.e., Hg, As, Se) are to be determined, precautions should be taken in the dissolution of SRM 2709 to avoid volatilization losses.

Statistical consultation was provided by S.B. Schiller of the NIST Statistical Engineering Division.

The overall direction and coordination of the analyses were under the chairmanship of M.S. Epstein and R.L. Watters, Jr., of the NIST Inorganic Analytical Research Division.

The technical and support aspects involved in the preparation, certification, and issuance of this Standard Reference Material were coordinated through the Standard Reference Materials Program by T.E. Gills and J.S. Kane.

Gaithersburg, MD 20899
October 30, 1992

William P. Reed, Chief
Standard Reference Materials Program

(over)

Instructions for Drying: When nonvolatile elements are to be determined, samples should be dried for 2 h at 110 °C. Volatile elements (i.e., Hg, As, Se) should be determined on samples as received; separate samples should be dried as previously described to obtain a correction factor for moisture. Correction for moisture is to be made to the data for volatile elements before comparing to the certified values. This procedure ensures that these elements are not lost during drying. The weight loss on drying has been found to be in the range of 1.8 to 2.5 %.

Source and Preparation of Material: The U.S. Geological Survey (USGS), under contract to the NIST, collected and processed the material for SRM 2709. The soil was collected from a plowed field, in the central California San Joaquin Valley, at Longitude 121° 25' and Latitude 36° 55'. The collection site is in the Panoche fan between the Panoche and Cantu creek beds. The top 7.5-13 cm (3-5 in) of soil containing sticks and plant debris was removed, and the soil was collected from the 13 cm level down to a depth of 46 cm (18 in) below the original surface. The material was shoveled into 0.114 m^3 (30-gal) plastic buckets and shipped to the USGS laboratory for processing.

The material was spread on 30.5 cm x 61 cm (1 ft x 2 ft) polyethylene-lined drying trays in an air drying oven and dried for three days at room temperature. The material was then passed over a vibrating 2-mm screen to remove plant material, rocks, and large chunks of aggregated soil. Material remaining on the screen was deaggregated and rescreened. The combined material passing the screen was ground in a ball mill to pass a 74-μm screen and blended for 24 h. Twenty grab samples were taken and measured for the major oxides using x-ray fluorescence spectrometry and for several trace elements using inductively coupled plasma atomic emission analysis to provide preliminary assessment of the homogeneity of the material prior to bottling. The material was bottled into 50-g units and randomly selected bottles were taken for the final homogeneity testing.

Analysis: The homogeneity, using selected elements in the bottled material as indicators, was assessed using x-ray fluorescence spectrometry and neutron activation analysis. In a few cases, statistically significant differences were observed, and the variance due to material inhomogeneity is included in the overall uncertainties of the certified values. The estimated relative standard deviation for material inhomogeneity is less than 1 % for those elements for which homogeneity was assessed.

Certified Values and Uncertainties: The certified values are weighted means of results from two or more independent analytical methods, or the mean of results from a single definitive method, except for mercury. Mercury certification is based on cold vapor atomic absorption spectrometry used by two different laboratories employing different methods of sample preparation prior to measurement. The weights for the weighted means were computed according to the iterative procedure of Paule and Mandel (NBS Journal of Research 87, 1982, pp. 377-385). The stated uncertainty includes allowances for measurement imprecision, material variability, and differences among analytical methods. Each uncertainty is the sum of the half-width of a 95 % prediction interval and includes an allowance for systematic error among the methods used. In the absence of systematic error, a 95 % prediction interval predicts where the true concentrations of 95 % of the samples of this SRM lie.

Table 1. Certified Values

Element	wt. %			Element	µg/g		
Aluminum	7.50	±	0.06	Antimony	7.9	±	0.6
Calcium	1.89	±	0.05	Arsenic	17.7	±	0.8
Iron	3.50	±	0.11	Barium	968	±	40
Magnesium	1.51	±	0.05	Cadmium	0.38	±	0.01
Phosphorus	0.062	±	0.005	Chromium	130	±	4
Potassium	2.03	±	0.06	Cobalt	13.4	±	0.7
Silicon	29.66	±	0.23	Copper	34.6	±	0.7
Sodium	1.16	±	0.03	Lead	18.9	±	0.5
Sulfur	0.089	±	0.002	Manganese	538	±	17
Titanium	0.342	±	0.024	Mercury	1.40	±	0.08
				Nickel	88	±	5
				Selenium	1.57	±	0.08
				Silver	0.41	±	0.03
				Strontium	231	±	2
				Thallium	0.74	±	0.05
				Vanadium	112	±	5
				Zinc	106	±	3

Noncertified Values: Noncertified values, shown in parentheses, are provided for information only. An element concentration value may not be certified if a bias is suspected in one or more of the methods used for certification, or if two independent methods are not available. Certified values for some of these elements will eventually be provided in a revised certificate when more data is available.

Table 2. Noncertified Values

Element	wt.%	Element	µg/g
Carbon	(1.2)	Cerium	(42)
		Cesium	(5.3)
		Dysprosium	(3.5)
		Europium	(0.9)
		Gallium	(14)
		Gold	(0.3)
		Hafnium	(3.7)
		Holmium	(0.54)
		Iodine	(5)
		Lanthanum	(23)
		Molybdenum	(2.0)
		Neodymium	(19)
		Rubidium	(96)
		Samarium	(3.8)
		Scandium	(12)
		Thorium	(11)
		Tungsten	(2)
		Uranium	(3)
		Ytterbium	(1.6)
		Yttrium	(18)
		Zirconium	(160)

Table 3. Analytical Methods Used for the Analysis of SRM 2709

Element	Certification Methods *	Element	Certification Methods *
Ag	ID ICPMS; RNAA	Mo	ID ICPMS
Al	XRF1; XRF2; INAA; DCP; ICP	Na	INAA; FAES; ICP
As	RNAA; HYD AAS; INAA	Nd	ICP
Au	INAA; FAAS	Ni	ID ICPMS; ETAAS; INAA
Ba	XRF2; FAES	P	DCP; COLOR; XRF2
C	COUL	Pb	ID TIMS
Ca	XRF1; XRF2; DCP	Rb	INAA
Cd	ID ICPMS; RNAA	S	ID TIMS
Ce	INAA; ICP	Sb	INAA; ETAAS
Co	INAA; ETAAS; ICP	Sc	INAA; ICP
Cr	INAA; DCP; ICP	Se	RNAA; HYD AAS
Cs	INAA	Si	XRF1; XRF2; GRAV
Cu	RNAA; FAES; ICP	Sm	INAA
Dy	INAA	Sr	ID TIMS; INAA; ICP
Eu	INAA	Th	ID TIMS; INAA; ICP
Fe	XRF1; XRF2; INAA; DCP	Ti	INAA; XRF1; XRF2; DCP
Ga	INAA; ICP	Tl	ID TIMS; LEAFS
Hf	INAA	U	ID TIMS; INAA
Hg	CVAAS	V	INAA; ICP
Ho	INAA	W	INAA
I	INAA	Y	ICP
K	XRF1; XRF2; FAES; ICP; INAA	Yb	INAA
La	INAA; ICP	Zn	ID TIMS; ICP: INAA; POLAR
Mg	INAA; XRF1; ICP	Zr	INAA
Mn	INAA; ICP		

*Methods in bold were used to corroborate certification methods or to provide information values.

ID TIMS - Isotope dilution thermal ionization mass spectrometry; mixed acid digestion.
ID ICPMS - Isotope dilution inductively coupled plasma mass spectrometry; mixed acid digestion.
INAA - Instrumental neutron activation analysis.
RNAA - Radiochemical neutron activation analysis; mixed acid digestion.
XRF1 - Wavelength dispersive x-ray fluorescence on fused borate discs.
XRF2 - Wavelength dispersive x-ray fluorescence spectrometry on pressed powder.
ICP - Inductively coupled plasma atomic emission spectrometry; mixed acid digestion.
DCP - Direct current plasma atomic emission spectrometry; lithium metaborate fusion.
ETAAS - Electrothermal atomic absorption spectrometry; mixed acid digestion.
CVAAS - Cold vapor atomic absorption spectrometry.
HYD AAS - Hydride generation atomic absorption spectrometry.
FAAS - Flame atomic absorption spectrometry; mixed acid digestion except for Au, leached with $HBr\text{-}Br_2$.
FAES - Flame atomic emission spectrometry; mixed acid digestion.
COLOR - Colorimetry; lithium metaborate fusion.
GRAV - Gravimetry; sodium carbonate fusion.
COUL - Combustion coulometry.
LEAFS - Laser enhanced atomic fluorescence spectrometry; mixed acid digestion.
POLAR - Polarography.

Participating NIST Analysts

M. Adriaens
E.S. Beary
C.A. Beck
D.S. Braverman
M.S. Epstein
J.D. Fassett
K.M. Garrity
R.R. Greenberg
W.R. Kelly
R.M. Lindstrom
E.A. Mackey
A. Marlow
J.R. Moody
P.J. Paulsen
P. Pella
T.A. Rush
J.M. Smeller
G.C. Turk
T.W. Vetter
R.D. Vocke
L.J. Wood
R.L. Watters, Jr.

Participating Laboratories

P. Briggs, D. Siems, J. Taggart, S. Wilson
U.S. Geological Survey
Branch of Geochemistry
Denver, CO 80225

J.B. Bodkin
College of Earth and Mineral Sciences
The Pennsylvania State University
University Park, PA 16802

S.E. Landsberger, V.G. Vermette
Department of Nuclear Engineering
University of Illinois
Urbana, IL 61801

National Institute of Standards & Technology

Certificate of Analysis

Standard Reference Material 99a

Soda Feldspar

This Standard Reference Material (SRM) is intended for use in the determination of constituent elements in feldspar or material of similar matrix. SRM 99a is powdered soda feldspar that was sieved to -200 mesh (75 μm) and blended to ensure homogeneity. The feldspar material came from Kona, North Carolina. Kona is within the Spruce Pine pegmatite district which has consistently been the principal producer of mica and feldspar.

The certified constituent elements of SRM 99a are given below and are based on measurements at NIST and a number of industrial laboratories. All values are based on samples that were dried for 2 hours at 105 °C.

Constituents	Certified Value[1] percent by weight
SiO_2	65.2^2
Al_2O_3	20.5
Fe_2O_3	0.06_5
TiO_2	0.007
CaO	2.14
BaO	0.26
MgO	0.02
Na_2O	6.2
K_2O	5.2
P_2O_5	0.02
Loss on Ignition	0.26

[1] The certified value listed for a constituent is the present best estimate of the "true" value. The certified values are given as the oxide on an equivalent weight basis and assume stoichiometry in the form of the compounds listed.

[2] The estimated uncertainty of a certified value is expressed in significant digits. The certified value listed is not expected to deviate from the true value by more than ± 1 in the last significant figure reported; for a subscript figure the deviation is not expected to be more than ± 5.

The original technical and support aspects involved in the preparation, certification, and issuance of this Standard Reference Material were performed under the direction of J.L. Hague of the Standard Reference Materials Program (formerly Office of Standard Reference Materials).

The revision and update of this Certificate of Analysis was coordinated through the Standard Reference Materials Program by T.E. Gills.

Gaithersburg, MD 20899
November 15, 1990
(Revision of certificates dated 3-26-65 & 8-10-81)

William P. Reed, Acting Chief
Standard Reference Materials Program

Bibliography

Barcelona, M. J. "Monitoring and Remediation: VOC Symptoms and Substance," Ground Water,: 4-5 (Spring 1993).

Bourg, Alain C. M., C. Mouvet, and, D.N. Lerner. "A review of the Attenuation of Trichloroethylene in Soils and Aquifers," Quarterly Journal of Engineering Geology, 25: 365-370 (1992).

Chiou, Cary T. "Roles of Organic Matter, Minerals, and Moisture in Sorption of Nonionic Compounds and Pesticides by Soils," Humic Substances in Soil and Crop Sciences 111-156 (1990).

Estes, Thomas J., R. V. Shah, and V. L. Vilker. "Adsorption of Low Molecular Weight Halocarbons by Montmorillite," Environmental Science and Technology, 22: 377-381 (April 1988).

Goltz, Mark N. "Analytical Modeling of Aquifer Decontamination by Pumping When Transport is Affected by Rate-Limited Sorption," Water Resources Research, 27: 547-556 (April 1991).

Laidler, K. J., Chemical Kinetics, Mcgraw-Hill, New York: 1965.

Lewis, T.E., A.B. Crockett, R.L. Siegrist, and K. Zarrabi. "Soil Sampling and Analysis for Volatile Organic Compounds," EPA 540/4-91/001: 1-24 (1991).

Lewis, Richard J., Sr. Sax's Dangerous Properties of Industrial Materials, Vol. 3. Rheinholt, New York: 1992.

Maliszewska-Kordybach, Barbara. "The Effect of Temperature on the Rate of Disappearance of Polycyclic Aromatic Hydrocarbons From Soils," Environmental Pollution: 15-21 (1992).

Masters, Gilbert M. Introduction to Environmental Science and Management. Prentice Hall, Englewood Cliffs, N.J.: 1991.

Ong, Say Key and L. W. Lion. "Mechanisms for Trichloroethylene Vapor Sorption onto Soil Minerals," Journal of Environmental Quality, 20: 180-188 (1991).

Pavlostathis, Spyros G. and Kendrick Jagial. "Desorptive Behavior of Trichloroethylene in Contaminated Soil," Environmental Science & Technology 25: 274-279 (1991).

Pavlostathis, Spyros G. and G. N. Mathavan. "Desorptive Kinetics of Selected Volatile Organic Compounds from Field Contaminated Soil," Environmental Science and Technology, 26: 532-538 (1992).

Pignatello, Joseph J. "Slowly Reversible Sorption of Aliphatic Halocarbons in Soils," Environmental Chemistry, 9: 1107-1115 (December 1990).

Reeder, Major Thomas L. Vadose Zone Contamination Measurements and Modeling. MS Thesis, AFIT/GEE/ENV/93S-13. School of Engineering, Air Force Institute of Technology (AU), Wright-Patterson AFB OH, September 1993 (AD-A270647).

Rogers, Robert D., J. C. McFarlane, and A. J. Cross. "Adsorption and Desorption of Benzene in Two Soils and Montmorillite Clay," Environmental Science and Technology, 14: 457-460 (April 1980).

Sadtler Research Laboratory, Sadtler Standard Infrared Grating Spectra. Sadtler Research Laboratory, Philadelphia: 1977.

Sawhney, J. J., and others. "Determination of 1,2-Dibromoethane (EDB) in Field Soils: Implications for Volatile Organic Compounds," Journal of Environmental Quality, 17: 149-152 (January 1988).

Serway, Raymond A. Physics for Scientists and Engineers / with Modern Physics. Saunders College Publishing, Chicago: 1983.

Siegrist, Robert L. "Volatile Organic Compounds in Contaminated Soils: The Nature and Validity of the Measurement Process," Journal of Hazardous Materials, 29: 3-15 (1992).

Smith, James A. "Effects of Soil Moisture on the Sorption of Trichloroethylene Vapor to Vadose Zone Soil at Picatinny Arsenal, New Jersey," Environmental Science and Technology, 24: 676-683 (May 1990).

Tognotti, Leonardo, Maria Fltyzani-Stephanopoulus, and Adel Fares Sarofim. "Study of Adsorption-Desorption of Contaminants on Single Soil Particles Using the Electrodynamic Thermogravimetric Analyzer," American Chemical Society, 25: 104-109 (January 1991).

Travis, Curtis C. and Jean M. Macinnis. "Vapor Extraction of Organics from Subsurface Soils," Environmental Science and Technology, 26: 1885-1887 (1992).

Vita

Captain Benjamin T. Kindt was born on 10 October 1967 in Tacoma, Washington. He graduated from Montgomery Catholic High School in Montgomery, Alabama in 1985 and attended the University of Notre Dame. In 1989 he graduated with a Bachelor of Science in Mechanical Engineering, was commissioned in the United States Air Force, and was assigned to the 67th Civil Engineering Squadron at Bergstrom AFB, Texas. As the mechanical engineer for the base he designed over $1 million worth of construction, maintenance, and repair projects during his first year. Next, he was assigned as Deputy Chief of Financial Management for the squadron and managed the budgeting and obligation of over $25 million representing nearly half of the entire base budget. In 1991, he was assigned as Deputy Chief of Environmental Management for the base. Over the next two years, he was responsible for every aspect of the environmental compliance and restoration of the base and managed the disposal of over a million pounds of hazardous waste annually. Also, while at Bergstrom AFB, he received a Master of Business Administration degree from Southwest Texas State University. In May of 1993, Captain Kindt was assigned to the Air Force Insitute of Technology to complete a Master of Science in Environmental Engineering degree.

REPORT DOCUMENTATION PAGE

Form Approved
OMB No. 0704-0188

1. AGENCY USE ONLY (Leave blank)	2. REPORT DATE	3. REPORT TYPE AND DATES COVERED
	September 1994	Master's Thesis

4. TITLE AND SUBTITLE
EXPERIMENT USING INFRARED SPECTROSCOPY TO STUDY THE EFFECT OF SOIL CHARACTERISTICS UPON THE RATE OF TRICHLOROETHYLENE DESORPTION

5. FUNDING NUMBERS

6. AUTHOR(S)
Benjamin T. Kindt, Captain, USAF

7. PERFORMING ORGANIZATION NAME(S) AND ADDRESS(ES)
Air Force Institute of Technology, WPAFB OH 45433-6583

8. PERFORMING ORGANIZATION REPORT NUMBER
AFIT/GEE/ENP/94S-02

9. SPONSORING/MONITORING AGENCY NAME(S) AND ADDRESS(ES)

10. SPONSORING/MONITORING AGENCY REPORT NUMBER

11. SUPPLEMENTARY NOTES

12a. DISTRIBUTION/AVAILABILITY STATEMENT
Approved for public release; distribution unlimited

12b. DISTRIBUTION CODE

13. ABSTRACT (Maximum 200 words)

This research investigated the influence of soil characteristics on the desorption of trichloroethylene (TCE). TCE is one of the most common contaminants at Superfund sites. Unfortunately, extraction of TCE from contaminated soils has been hindered by its slow and poorly understood desorption from soil particles. The rate and progress of desorption of TCE from seven types of soil with varying particle diameters and elemental compositions was measured using optical absorption techniques. Fitting the data to the Langmuir Isotherm functional form predicted in the literature yielded parameters for the desorption rate and total amount of desorption from each soil type. These parameters were compared to the characteristics of the soil samples to determine if any correlation existed. Soil characteristics appeared to have a significant influence on the desorption of TCE. Both the rate of desorption and the total amount of desorption showed a strong negative correlation with the particle diameter of the soils. Additionally, the elemental composition of the soil appeared to have a significant effect on the desorption phenomena.

14. SUBJECT TERMS
Trichloroethylene, Environment, Optics, Restoration, Desorption, Soil

15. NUMBER OF PAGES
89

16. PRICE CODE

17. SECURITY CLASSIFICATION OF REPORT	18. SECURITY CLASSIFICATION OF THIS PAGE	19. SECURITY CLASSIFICATION OF ABSTRACT	20. LIMITATION OF ABSTRACT
Unclassified	Unclassified	Unclassified	UL